ECOSYSTEMS

ORIGINAL ARTICLE

Mapping the Spatial Heterogeneity of Watershed Ecosystems and Water Quality in Rainforest Fjordlands

Ian J. W. Giesbrecht,[1]* Ken P. Lertzman,[2] Suzanne E. Tank,[3] G. W. Frazer,[4] Kyra A. St. Pierre,[5] Santiago Gonzalez Arriola,[6] Isabelle Desmarais,[7] and Emily Haughton[7]

[1]Hakai Institute and Simon Fraser University, Vancouver, British Columbia, Canada; [2]Simon Fraser University and Hakai Institute, Vancouver, British Columbia, Canada; [3]University of Alberta and Hakai Institute, Edmonton, Alberta, Canada; [4]GWF LiDAR Analytics and Hakai Institute, Sidney, British Columbia, Canada; [5]University of Ottawa and Hakai Institute, Ottawa, Ontario, Canada; [6]Hakai Institute, La Paz, Baja California Sur, Mexico; [7]Hakai Institute, Campbell River, British Columbia, Canada

ABSTRACT

Small coastal watersheds ($< 10,000$ km^2) can play a large role in forming biogeochemical linkages between land and sea, yet the spatial heterogeneity of small watershed ecosystems is poorly understood due to sparse observations in many regions. In this study, we examined the spatial heterogeneity of water quality exported from diverse watersheds in two rainforest fjordland complexes. Samples were collected about monthly for a year from the outlets of 56 watersheds spanning from high mountains to low islands. Many (20) water quality properties varied significantly across six previously established watershed types defined by 12 easily computed geospatial variables. For example, organic matter concentrations ranged from very low in a Glacierized Mountains watershed type (1.2 ± 0.1 mg L^{-1} DOC; 28.5 ± 4.6 µg L^{-1} DON) to very high (15.1 ± 1.0 mg L^{-1} DOC; 215.6 ± 20.4 µg L^{-1} DON) in a Rain Lowlands type. Along this gradient, the dominant form of dissolved nitrogen switched from inorganic to organic and the dominant form of phosphorous switched from particulate to dissolved. Watershed type alone explained 67% of the variance in the first principal component of water quality (PC1) representing 20 water properties. Although underlying causes were likely complex, a great deal of spatial variation in water quality (for example, 91% of PC1) was predicted by simple measures of topography and climate (for example, elevation and mean annual precipitation). The physiographic structure of the coastal land mass appears to enable a complex mosaic of watershed ecosystems, which may affect meta-ecosystem function at the coastal margin.

Key words: Watersheds; Watershed ecosystems; Biogeochemistry; Landscape; Ecology; Meta-ecosystems; Rainforest; Fjord; Carbon; Nutrients; Glaciers.

Highlights

- The quality of freshwater exports to the ocean varied significantly across watersheds
- Spatial variation in water quality can be predicted by easily measured watershed characteristics
- Spatial heterogeneity of riverine water quality may have ecosystem effects at the fjordland scale

Introduction

Small coastal watersheds ($< 10,000$ km^2) can play a large role in the export of terrestrial materials to the ocean (Lyons and others 2002; Milliman and Syvitski 1992; McNicol and others 2023). However, the spatial heterogeneity among small coastal watershed ecosystems is significant and understudied in the scientific literature. This hinders our ability to understand how and why freshwater ecosystems and the land–ocean aquatic continuum (Xenopoulos and others 2017) vary among drainages. Measurements of riverine water quality—which we use as an umbrella term for physical and biogeochemical measurements of aquatic ecosystems—tend to be sparse and unevenly distributed across the diversity of small coastal watersheds (for example, Milliman and Farnsworth 2011). Furthermore, many studies of small coastal watersheds report only one or a few aspects of riverine water quality, limiting our opportunities to understand the *watershed ecosystem* (Bormann and Likens 1967) as an integrator of within-catchment complexity (Likens 2001).

The concept of a *spatial mosaic* has long been used by landscape ecologists in their efforts to understand the interactions of spatial heterogeneity and ecosystem processes (Levin 1992; Pickett and Cadenasso 1995; Turner 1989; Wiens 2002). Spatial variation in riverine water quality can be used to better understand the processes that control losses from watershed ecosystems (for example, Borman and Likens 1967; Stewart and others 2021). Drawing from foundations in landscape ecology and ecosystem science, the *meta-ecosystem* concept describes "a set of ecosystems connected by spatial flows of energy, materials and organisms across ecosystem boundaries." (Loreau and others 2003 p. 674; Gounand and others 2018). These theoretical concepts may be useful for understanding land–sea linkages in regions characterized by abundant small coastal watersheds. However, many regions lack the spatially explicit modeling frameworks and the well-distributed field data needed for theoretical and applied studies of *hydro-biogeochemistry* over large areas and multiple scales (Li and others 2021).

Illustrating all of these problems, the extensive fjordlands of the world (Bianchi and others 2020) are often characterized by strong spatial gradients from mountainous inlets to islands of comparatively low elevation. In coastal temperate rainforest regions such as the Northeast Pacific Coastal Temperate Rainforest (NPCTR) and Chilean Patagonia, these fjordland complexes have very diverse watershed characteristics ranging from glacierized mountains to low-lying peatlands (Giesbrecht and others 2022; Vargas and others 2011). However, published observations of riverine water quality in these settings are sparse and typically limited in scope. For example, the sampling of fjord inputs tends to focus on the largest watersheds while the water quality of many smaller watersheds remains undescribed. Furthermore, while dissolved organic carbon has been studied intensively in a few watersheds of the NPCTR fjordlands (for example, Fellman and others 2009; Oliver and others 2017) and modeled over regional scales (Edwards and others 2021; McNicol and others 2023), nitrogen, phosphorous, iron, and other micronutrients remain understudied across this large and diverse region (Bidlack and other 2021; but see examples in Fellman and others 2021; Hood and Berner 2009; St. Pierre and others 2021). Watershed classification for hydro-biogeochemistry can be a useful tool for mapping and modeling spatial heterogeneity over such poorly sampled areas (Li and others 2021; Ouellet Dallaire and others 2019; Snelder and Biggs 2002; Wolock and others 2004). One such classification has been validated for streamflow regimes and dissolved organic carbon (DOC) dynamics in this NPCTR region but has not been validated with other aspects of water quality (Giesbrecht and others 2022).

Across forested watersheds, topography, climate, vegetation, soils, lithology, and management are among the main spatial controls on riverine water quality (for example, Bormann and Likens 1967; Gibbs 1970; Mendoza-Lera and others 2021; Lintern and others 2018; Tank and others 2012a). This reflects the dependence of water quality on the structure, composition, and processes of Earth's critical zone—the vertical zone from vegetation canopy to permeable bedrock—including the hydrologic flowpaths, reactivities, conductivities, and residence times within that zone (Anderson and others 2007; Chorover and others 2017; Richter and Billings 2015). For example, watershed relief is often found to be a major control on the

biogeochemistry of freshwater ecosystems (for example, Mulholland 2003; Sobek and others 2007), but not always (for example, Gaillardet and others 1999). Watershed climate is also a control on both catchment hydrology (for example, Curran and Biles 2021) and stream biogeochemistry (Aitkenhead-Peterson and others 2005; White and others 1999). The relative cover of Alder (*Alnus spp.*) in a watershed can be a major control on the concentration of dissolved organic nitrogen (DON) and thus (after mineralization) dissolved inorganic nitrogen (DIN) in streams (Compton and others 2003; Steinberg and others 2011), potentially reflecting logging legacies and forest seral stage (Cairns and Lajtha 2005). More broadly, riverine water quality is affected by a wide range of environmental policies and management decisions (for example, Sergeant and others 2022; Shah and others 2022; Williamson and others 2008). However, forestry is particularly relevant in the central to northern NPCTR given the prevalence of this land use.

Glaciers also exert strong controls on riverine water quality and quantity (Moore and others 2009) thereby creating ecosystem linkages from icefields to ocean (O'Neel and others 2015). Downstream water quality is affected by physical grinding and chemical weathering processes (Anderson 2007; Tranter and Wadham 2014), seasonal melting of glacial ice and snow (Hood and Berner 2009; O'Neel and others 2015; Hodgkins and other 1997), biologically active glacier ecosystems (Hodson and others 2008; Ren and others 2019), and the absence of terrestrial vegetation and soil organic matter (Hood and Berner 2009; Milner and others 2017). As a result of glacial processes, spatial gradients of increasing watershed glacier cover are associated with predictable spatial gradients in many aspects of riverine water quality, including organic matter, certain inorganic nutrients, rock weathering products, temperature, and turbidity (Brahney and others 2021; Fellman and others 2014a, b; Hood and Berner 2009; Moore and others 2009; Milner and others 2017). For instance, particulate and soluble reactive phosphorous (SRP) concentrations tend to increase with watershed glacier cover. However, other glacier effects are less consistent across studies. For example, DIN concentrations can either decrease (Hood and Berner 2009; Milner and others 2017) or increase with glacier cover (Colombo and others 2019; Slemmons and others 2013; Warner and others 2017), depending on the region. Within the NPCTR region, numerous studies examine the effects of glaciers on water quality in Southeast Alaska, yet very little has been done to test these ideas in the glacierized fjords of central and south-central British Columbia.

In this study, we examined the spatial heterogeneity of small coastal watershed ecosystems across two rainforest fjordland complexes of the central NPCTR region in British Columbia, considering a broad range (22) of riverine water quality properties. The watersheds varied dramatically in terms of topography, climate, glacier cover, and vegetation, while lithology was held comparatively constant. We hypothesized that physiographic complexity would generate significant spatial heterogeneity of both watershed and water quality characteristics. Furthermore, we hypothesized that a small number of watershed types defined by readily available geospatial data (Giesbrecht and others 2022) would represent a meaningful amount of the spatial variation in multiple aspects of riverine water quality. Finally, we explored the relative importance of specific climatic and topographic watershed characteristics for predicting riverine water quality at the coastal margin.

Methods

Study Area and Sampling Design

We studied 56 watersheds spanning diverse environmental settings from high-mountain icefields to low islands (Figure 1). Watershed size ranged from < 1.5 km² to 5,782 km² (Homathko River), yet in the regional and global context, all are considered "small" coastal watersheds (< 10,000 km² following Milliman and Syvitski, 1992). The study watersheds were spatially distributed along two fjordland transects on the south-central coast of British Columbia, Canada (51°57′ N to 50°07′ N and 128°09′ W to 123°44′ W). Located in the Perhumid rainforest zone (Alaback 1996; Wolf and others 1995) at the northern end of the study area, the Rivers Inlet transect (*n* = 31 watersheds; Figure 1) spans from Calvert Island in the west to the Wannock watershed at the head of Rivers Inlet. In the Seasonal Rainforest zone (Alaback 1996; Wolf and others 1995; Figure 1) at the southern end of the study area, the Bute Inlet transect (*n* = 25 watersheds) spans from Quadra Island in the southwest to the Homathko watershed at the head of Bute Inlet.
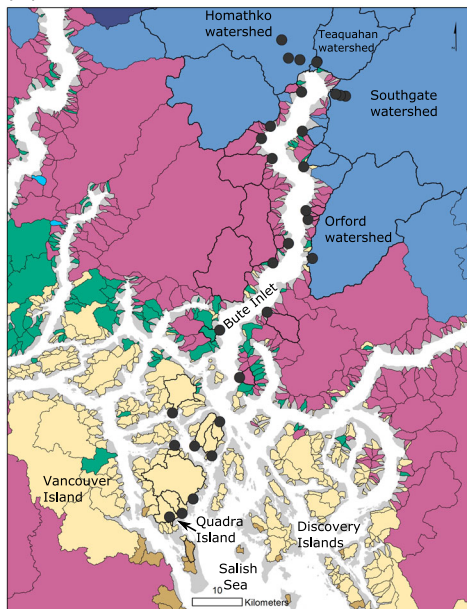
Both study transects are broadly similar in lithology to the rest of the mainland coast of BC and the Coast Mountains along the border of Southeast Alaska and British Columbia (Figure S1). This large geological region—known as the Coast
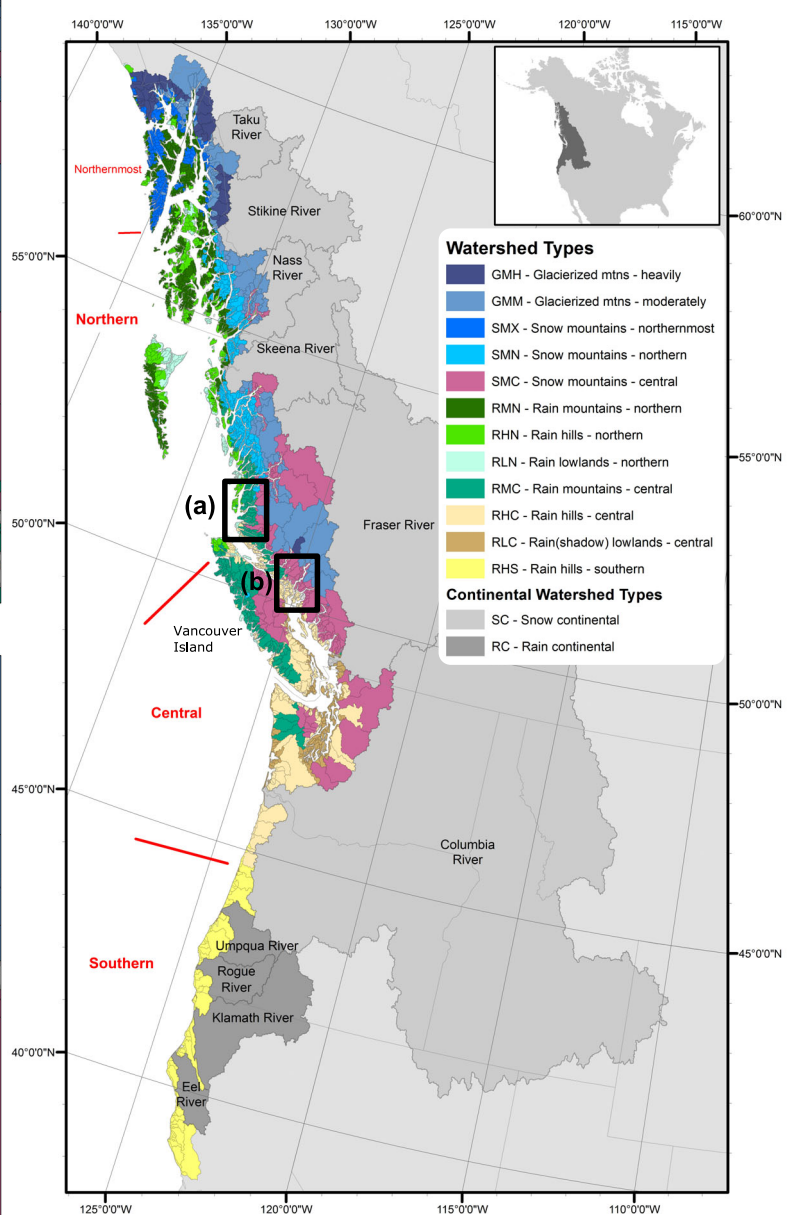
(a) Rivers Inlet transect
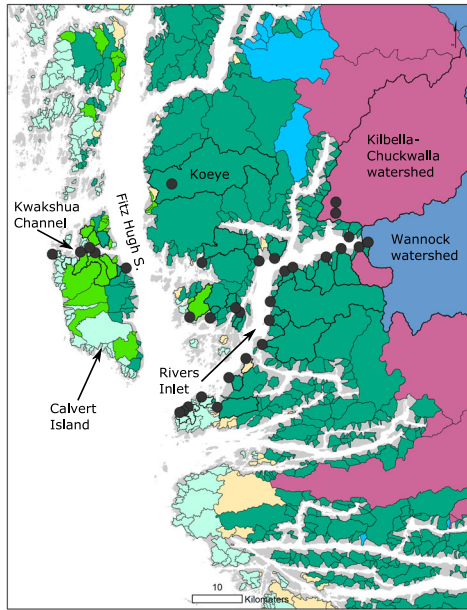
(b) Bute Inlet transect

(c) Regional context

Figure 1. Watersheds of the study area **a** and **b**, in the context of regional-scale spatial gradients of watershed diversity **c**. Black boxes in **c** indicate the locations of the fjord-scale maps in the region. Black dots in **a** and **b** indicate the locations of 56 river outlets where we collected water quality measurements for this study. Watershed color indicates watershed type, as defined in the legend for **c**. Fjord scale watershed types in **a** and **b** were predicted using random forest modeling in this study, with a random forest out-of-bag (OOB) error rate of 9.27%. Note that the largest watersheds extend beyond the inset panels in **a** and **b**. The regional map **c** and the names of watershed types are from Giesbrecht and others (2022).

Plutonic Complex or Coast Mountains Batholith (Rusmore and Woodsworth 1991; Cecil and others 2018)—is predominantly plutonic rock and some metamorphic rock, with only small pockets of sedimentary and volcanic rock (Table S1; Figure S1; Garrity and Soller 2009; Hartmann and Moosdorf,

2012; Stowell, 2006). This contrasts with the rest of the NPCTR, where sedimentary or volcanic rocks are dominant (for example, Vancouver Island and the island archipelago of Southeast Alaska). However, a few watersheds at the southern end of the Bute Inlet transect are in the transition from the

Coast Plutonic Complex to the volcanic rock of Vancouver Island (Figure S1a) and were omitted from most of our analyses (see below). Substantial deposits of Quaternary sediment occur in valley bottoms of the larger watersheds and some low-elevation areas along the outer coast (Cui and others 2017).

The study area has a rainforest climate with large amounts of orographic precipitation produced as moist Pacific air masses move onto the continent, especially in fall and winter months (Demarchi 2011). However, a rainshadow occurs in the lee of the Vancouver Island mountains, with the greatest effect in the southwestern part of our study area (the Discovery Islands) where precipitation is lower and summers are warmer (Wang and others 2016). The Coast Mountains in and around this study area hold North America's largest glaciers south of Alaska (for example, Ha-Iltzuk Icefield and Homathko Icefield).

Terrestrial ecosystems of the study area are typical of coastal temperate rainforest (Alaback 1996) yet vary dramatically across the study area. Podzolic soils are widespread, with high organic matter content and low pH (Sanborn and others 2011). The hypermaritime outer coast (for example, Calvert Island; Figure 1) is characterized by extensive open wetlands and low productivity bog forests (Banner and others 2005; Thompson and others 2016). Terrestrial productivity is much higher in the Discovery Islands and at low elevations of the mainland coast, while slow growing forests and alpine meadows are found at higher elevations (Meidinger and Pojar 1991; Pojar and others 1991). The overall soil landscape mosaic thus has high soil organic carbon stocks in the global context (McNicol and others 2019). However, exposed bedrock is common: in the alpine, in very steep terrain, in recently deglaciated areas, and within the lower elevation bog-forest mosaic of the outer coast (Meidinger and Pojar 1991). Exposed sediment is common in recently deglaciated areas and in alluvial systems downstream of glaciers.

Humans have used this area for millennia, yet the watershed ecosystems of this study area are less impacted by development than many watersheds found further south in the NPCTR (Wolf and others 1995). Indigenous people have continuously occupied this area for at least 13,000 years (McLaren and others 2018), using and managing resources from land to sea (for example, Dick and others 2022; Hoffman and others 2017; Jackley and others 2016; Reid and others 2022). At present, some of the study watersheds include small rural communities, but there are no urban areas. Old-growth and mature forests are still dominant in many areas, yet early- and mid-seral stages are common, particularly in productive valley bottoms (Benner and Lertzman 2022; Pearson 2010) and in the south (Old Growth Technical Advisory Panel 2021a; b). Agricultural activities are limited and no major polluting industries, mines, or hydro development projects are located within the watersheds. However, marine traffic passes nearby and regional sources of emissions are found within the Salish Sea airshed (Aherne and others 2010; Hember 2018).

Watershed Characterization and Classification

This study takes advantage of a previous watershed classification effort, which used four widely available (open access) datasets and 12 easily computed watershed characteristics (Table 1) to define 12 types of small coastal watersheds with cluster analysis (Giesbrecht and others 2022). These clusters separated watersheds by characteristic water source (glacial, snowmelt, rain), topography (mountains, hills, lowland), climate and geographic location within the NPCTR (north, central, south). Watershed types were validated with riverine field observations and found to represent a wide range of contrasting streamflow regimes and DOC concentration and seasonality. In this previous effort, Giesbrecht and others (2022) developed the hypothesis that watershed classification for hydrobiogeochemistry would be useful for characterizing the spatial gradients of many other aspects of riverine water quality.

For the present study, we assigned every sampled watershed to one of the 12 types of coastal watershed defined in Giesbrecht and others (2022). This assignment required a modeling step because 34 of our 56 sampled watersheds were smaller than the minimum size (20 km^2) of well-delineated watersheds (DW) used in the regional-scale classification (2022; Figure S2). We used a random forest (Breiman 2001) classifier (*randomForest* package v4.6.14; Liaw and Wiener 2002) in R Statistical Software (R Core Team 2020) to assign class membership to newly delineated (< 20 km^2) watersheds. The predictor variables were the 12 watershed characteristics (Table 1) originally used to define the regional watershed types via cluster analysis (Giesbrecht and others 2022). The response variable was watershed type. The model was trained using the $n = 669$ DW that appear in both the regional dataset and the BC Freshwater Atlas dataset. We used 500 trees and three randomly selected

Table 1. Characteristics of the Sampled Watersheds Grouped by Watershed Type

Type WType	Centroid x location Poly_x	Centroid y location Poly_y	Glacier cover (%) Glc_prct	Max elev (m) Elev_max	Slope (°) Slpe_avg	Slope < 5° (%) Slpe5	MAP (mm) MAP	PAS (mm) PAS	MAT (°C) MAT	TD (°C) TD	Eref (mm) Eref	Veg Ht (m) VegHt	Area (km²) Area_km2	n
RHC	− 1,955,555	1,531,185	0.0	557	15.3	12.9	2,041	151	8.5	15.0	610	29.8	18	9
	(35,776)	(61,797)	(0.0)	(164)	(3.5)	(6.0)	(408)	(38)	(0.4)	(1.3)	(37)	(2.1)	(21)	
RLN	− 2,065,639	1,696,937	0.0	172	9.4	30.4	2,889	102	8.6	10.3	487	25.8	3	5
	(6868)	(17,482)	(0.0)	(59)	(2.1)	(11.0)	(31)	(6)	(0.1)	(0.2)	(9)	(4.5)	(1)	
RHN	− 2,067,201	1,721,684	0.0	620	14.6	12.6	3,543	183	8.1	11.2	510	23.1	11	4
	(8598)	(8174)	(0.0)	(281)	(2.7)	(2.7)	(257)	(55)	(0.3)	(0.3)	(9)	(3.4)	(6)	
RMC	− 2,036,102	1,700,026	0.0	1,018	23.2	4.4	3,448	400	6.8	12.4	501	27.7	28	19
	(27,527)	(41,746)	(0.0)	(395)	(6.0)	(3.5)	(318)	(209)	(1.0)	(0.9)	(21)	(3.2)	(46)	
SMC	− 1,930,960	1,582,090	1.8	1,854	33.3	1.1	2,916	903	4.8	15.7	491	21.5	87	11
	(41,819)	(69,057)	(3.2)	(295)	(5.0)	(1.3)	(505)	(260)	(0.9)	(0.8)	(36)	(5.8)	(210)	
GMM	− 1,901,358	1,592,476	18.1	2,919	31.0	3.8	2,737	1,377	2.4	16.3	426	12.5	1,577	8
	(33,509)	(50,100)	(8.8)	(491)	(5.2)	(3.3)	(588)	(165)	(0.9)	(0.6)	(21)	(4.0)	(2,182)	

Acronyms for watershed types are defined in Fig. 1. The first 12 numeric data columns give the 12 watershed properties used for watershed classification. Summary statistics represent the watershed mean (and standard deviation). The variables were defined as follows: centroid x and centroid y location = watershed centroid coordinates; glacier cover = % cover of glaciers; max elev = maximum watershed elevation; slope = average watershed slope; slope < 5° = the proportion of the watershed with slope < 5°; MAP = mean annual precipitation; PAS = precipitation as snow; MAT = mean annual temperature; TD = temperature difference between mean warmest month temperature and mean coldest month temperature (a measure of continentality); Eref = Hargreaves reference (potential) evaporation Veg Ht = mean vegetation height. This table also reports mean watershed area (Area) and total number of polygons sampled for stream biogeochemistry (n).

candidate variables at each split. Re-running the analysis with 5,000 trees did not change the predicted watershed type for any of the 56 sampled watersheds. The present analysis revised the previous regional watershed classification (Giesbrecht and others 2022) by better resolving the locations and extent of watersheds in the $\sim$ 1 to 10 km^2 size range (Figure 1; Figure S2), particularly those with very low relief and extensive wetland cover (see Supplemental Information, Text S1). Despite this, we suspect that a small number of watersheds were misclassified by the RF model (see Text S1) thereby contributing some noise to our analysis of water quality across types.

Our watershed classification required a dataset of watershed boundaries and catchment characteristics. To produce this dataset, we generated a polygonal shapefile of coastal watersheds derived from the BC Freshwater Atlas ''assessment'' watersheds (GeoBC 2009). We defined watersheds according to their outlets to the ocean, which required amalgamation of all subcatchments to a single polygon in GIS. Each watershed polygon was then characterized by 12 watershed properties expected to control or predict river hydrology and water quality (Table 1). See (Giesbrecht and others 2022) for detailed methods. For the present study, we used the same procedures and the same data (e.g., vegetation height from Simard and others, 2011), with three exceptions. First, we used a higher resolution (25 m instead of $\sim$ 90 m) digital elevation model (TRIM; GeoBC 2014). Second, we used an updated version of the Randolph Glacier Inventory (v6.0 instead of v5.0; RGI Consortium 2017). Third, we used an updated version of ClimateNA (v6.22 instead of v5.10) (Wang and others 2016; AdaptWest Project 2020).

In addition to the 12 variables used in prior watershed classification, we measured several other watershed characteristics that could affect water quality and interpretation. To represent potential geological effects, we quantified the percentage watershed cover of lithological classes (Moosdorf and Hartmann 2015) and of Quaternary sediments (Cui and others 2017). To represent land cover and forest disturbance, we quantified the percentage forest cover of four seral stages; early-seral, mid-seral, mature forest, and old forest (Old Growth Technical Advisory Panel 2021b). The remainder of each watershed was considered non-forest. We also computed the percentage cover of waterbodies (lakes and rivers) in each watershed (GeoBC 2008).

We estimated the cumulative extent and approximate discharge of each watershed type be-

tween the northern and southern extent of our field study (Figure 1). The area of each watershed type was summed using ArcGIS (Esri 2020) for all land between the Koeye watershed (Figure 1a) and Bute Inlet (Figure 1b), including Vancouver Island, the mainland, and all small islands in between. Cumulative annual discharge from each watershed type was then estimated by multiplying the average of mean annual runoff (MAR; discharge per unit area) reported in an earlier regional study (Giesbrecht and others 2022) by the area of each watershed type in this study area. For the three largest watersheds, we used the MAR calculated from local gauge data in Giesbrecht and others (2022).

Stream Chemistry Data

Water samples were collected from the watershed outlets roughly once every month for a year (March 2018 to March 2019), for a total of 405 observation site-days after quality control. Most watersheds were sampled eight to ten times. Each transect was surveyed over two to three consecutive days to sample under relatively similar weather and flow conditions. The two transects were surveyed as close together in time as feasible, but were often more than a week apart, thus not always capturing the same weather system.

From each water sample, we measured 22 aspects of riverine water quality, including DOC, alkalinity, cations, organic and inorganic nutrients, δ^{18}O-H$_2$O, δ^2H-H$_2$O, and handheld sensor (YSI ProDSS) readings of temperature, specific conductance, pH, and turbidity. Water samples and sensor readings were taken from the main flow, avoiding eddies, shallow water, loose substrates, or woody debris. Samples for dissolved constituents were field filtered with a 0.45-μm Millipore® Millex-HP hydrophilic polyethyl sulfonate (PES) syringe filter. All samples were kept cool and dark during the field work. Samples were then preserved by freezing or acidification as appropriate, within 24 h of field collection. The field and laboratory procedures for this study follow those of St. Pierre and others (2021) and Tank and others (2020). Laboratory results below the detection limit were replaced by ½ the detection limit, following common convention (for example, EPA 2000). In addition to direct measurements, we calculated several variables from the analytical laboratory results: the total concentration of DIN, DON, particulate nitrogen (PN) dissolved organic phosphorous (DOP), and particulate phosphorous (PP). PN was calculated by subtracting total dissolved nitrogen (TDN) from

total nitrogen (TN) and PP was calculated by subtracting total dissolved phosphorous (TDP) from total phosphorous (TP). Finally, we computed the mass ratio of sodium to calcium ions (Na:Ca) as a simple index of cation origin. High Na:Ca ratios can be caused by high inputs of cyclic marine salts (via precipitation) relative to cation inputs from rock weathering (Gibbs 1970; Schlesinger 1997) and by high inputs from silicate weathering relative to carbonate weathering (Gaillardet and others 1999; Tank and others 2012a).

Several quality control (QC) and data cleaning procedures were implemented prior to the analysis, using a combination of visual inspection and data-based criteria. For visual inspection, tables and plots of the water quality measurements were examined while cross-referencing metadata from field notes and laboratory notes. We omitted any suspiciously high or low values that could be readily explained by a procedural anomaly such as a cracked sample vial. For data-based QC, outlier values of sensitive species (DIN species, TN, and SRP) were identified (mean $\pm$ 4SD) and omitted unless supported by independent measurements (for example, high DIN supported by high TDN and high TN). Additional quality control procedures were applied to calculated values to avoid use of illogical results. For example, where DIN > TDN, the resulting negative DON value was replaced with ½ the detection limit of TDN to indicate a small non-zero quantity. We also omitted samples where specific conductance exceeded 200 μS cm^{-1}, which are suspiciously high for the geological conditions we sampled. These samples also had high concentrations of Na^+, K^+, Cl^-/SO_4^{2-}, or Sr^{2+} (where available), likely due to tidal mixing of brackish water. We identified seven such cases, representing five site-dates.

We checked how well the sampling dates represented the distribution of flow conditions observed at 12 representative streamflow gauges during the study period. Although most of the study streams are not gauged, we were able to identify between one and three representative gauges for each watershed type (Table S2). We considered all streamflow gauges operated by the Water Survey of Canada and the Hakai Institute as candidates. Gauges were selected based on similarity of watershed characteristics known to predict streamflow regimes in this region (Giesbrecht and others 2022) including watershed elevation, mean annual precipitation, evaporation, and glacier cover. Where available, we included gauges with contrasting levels of lake cover or glacier cover in the same watershed type and selected gauges from across the area of interest for better geographic representation. For example, we selected two RHN gauges at the Kwakshua Watersheds Observatory—one with and one without major lake effects—and one RHN gauge much further south on Vancouver Island. After compiling discharge data from the selected gauges using the *tidyhydat* package (Albers 2017) in R for Water Survey of Canada stations and a published dataset from the Hakai Institute (Korver and others 2022), we computed daily specific discharge for each gauge and the average daily specific discharge for each watershed type. We then compared the distribution of sampled flows with the distribution of all flows using visual comparisons (hydrographs and boxplots) and a two-sample Kolmogorov–Smirnov (K-S) test.

To evaluate the broad seasonality of stream chemistry, we defined two seasons based on the dominant sources of runoff to streams. A *rain-driven season* typically occurs from October through April, when streamflow events are dominated by rainfall inputs at lower to middle elevations. This is the high flow season in Rain type watersheds and the low flow season in Glacierized watershed types, where cold winter temperatures cause precipitation to fall as snow (Giesbrecht and others 2022). A *meltwater season* typically occurs from May through September, when the Glacierized Mountain watersheds tend to have high yields of meltwater (snow and glacier-dominated streamflow). Precipitation reaches a minimum during this season, resulting in low flows for rain-dominated watersheds.

The water quality dataset was handled in two different ways to accommodate two different objectives. In Phase 1, the full water quality dataset (56 watersheds and n = 405 site-days) was used for principal components analysis (PCA) analysis and a heatmap because our primary goal was to describe correlations among water quality variables over both space and time. In Phase 2, where our goal was to compare water quality across watersheds, we used more restrictive watershed selection criteria. Specifically, we controlled for major lithological effects on stream chemistry (Hartmann and others 2014; Jansen and others 2010; Milliman and Farnsworth 2011) by considering only watersheds dominated by the plutonic–metamorphic lithology that characterizes the BC mainland coast (Figure S1). Three watersheds with > 50% combined cover of sedimentary or volcanic lithology were removed. The remaining watersheds all had more than about 75% cover of plutonic and/or metamorphic rock (Table S1). In the Phase 2 dataset, we also eliminated watersheds with fewer than three

sampling dates to avoid a potentially biased estimate of typical stream chemistry in a given watershed. Eight watersheds were eliminated on this basis leaving a total of 45 watersheds for the Phase 2 analyses. Finally, in Phase 2 we used the average biogeochemistry of all temporal observations in each watershed, except where our goal was to characterize seasonality.

Statistical Analysis of Stream Biogeochemistry Data

We used PCA to reduce the high dimensionality of the water quality dataset into a smaller number of synthetic (principal) components. PCA was computed by a singular value decomposition of a centered and scaled data matrix using the *prcomp()* function in R (*stats* package; R Core Team 2020). We constructed a biplot of principal component scores (points) and loadings (vectors) in the reduced feature space of the first two principal components to visualize biogeochemical differences and similarities among sites within and between watershed types. We omitted turbidity from the PCA because the large number of missing values would have substantially reduced the sample size.

We used a combination of summary statistics and statistical tests to evaluate biogeochemical differences across watershed types. Boxplots were used to describe the distribution and median value of stream observations in each watershed type and across seasons. We used a one-way analysis of variance (ANOVA) to determine if the watershed types had statistically significant mean differences in stream biogeochemistry.

We used random forest (RF) regression (Breiman 2001) via the *randomForest* package (v4.6.14; Liaw and Weiner 2002) in R to estimate how much of the observed spatial variation in stream biogeochemistry could be explained by watershed type, the 12 watershed properties used to define watershed types, lithology, forest cover, as well as all these candidate variables combined. We generated 5,000 trees in each forest to ensure stable results and randomly selected p/3 variables at each split, where p is the number of candidate variables. The RF analysis was done at the scale of individual watersheds using the temporally averaged chemistry of each watershed. We also used RF to quantify and rank the relative importance of the 12 watershed classification variables as well as several measures of watershed lithology and forest cover for predicting stream biogeochemistry at the catchment scale. We used these RF results in combination with our other findings to identify two key predictor variables that appeared to account for a large fraction of the observed catchment controls on stream biogeochemistry. To visualize and quantify the strength of these controls, we constructed generalized additive models (GAM) with the Gaussian family of distributions using the *mgcv* package in R (v1.8.31; Wood 2011, 2017). Smoothing parameters were automatically selected using the restricted maximum likelihood (REML) method.

RESULTS

The watershed classification analysis showed that six watershed types dominated the two fjordland transects (Figure 1). The 56 watersheds we sampled for riverine water quality varied along a multi-attribute environmental gradient (Table 1) from Rain (R) to Glacierized (GMM) watershed types, which reflected increasing elevation and size, decreasing mean annual air temperature, increasing snowfall and glacier cover, decreasing vegetation height, and decreasing proximity to the coastal ocean (beyond fjord waters). Rain-fed watersheds were diverse, with four different types across the two transects. The three Rain types in the Rivers Inlet area varied along a topographic gradient from Rain Lowlands (RLN) to Rain Hills (RHN) to Rain Mountains (RMC), with increasing slope (from $9.4 \pm 2.1°$ to $23.2 \pm 6.0°$) and decreasing extent of flat areas (from $30.4 \pm 11.0\%$ to $4.4 \pm 3.5\%$ slope $< 5°$) across that gradient. The Rain Hills type found on the Bute Inlet transect (RHC) had much lower precipitation ($2,041 \pm 408$ mm) and taller vegetation (29.8 ± 2.1 m) than the Rain Hills type of the Rivers Inlet transect (RHN; $3,543 \pm 257$ mm and 23.1 ± 3.4 m), due to the rainshadow of Vancouver Island. In fact, all watersheds of the Bute Inlet transect had lower precipitation than watersheds of the Rivers Inlet transect with a similar elevation (Figure S3a). The RHC watershed type also had a much higher proportion of mid- and early-seral forest cover—and a lower proportion of old forest cover—compared other watershed types (Figure S4). Non-forest cover was very high in the GMM ($> 75\%$), SMC ($> 50\%$), and RHN ($\sim 50\%$) type watersheds (Figure S4). Waterbody cover was higher in Rain Hills and Lowlands than in the Mountain type watersheds (data not shown).

Streamflow regimes differed across watershed types (Figure 2) as expected from a prior regional-scale analysis that included this study area but not the KWO gauges (Giesbrecht and others 2022). Spring freshet signals were pronounced in the
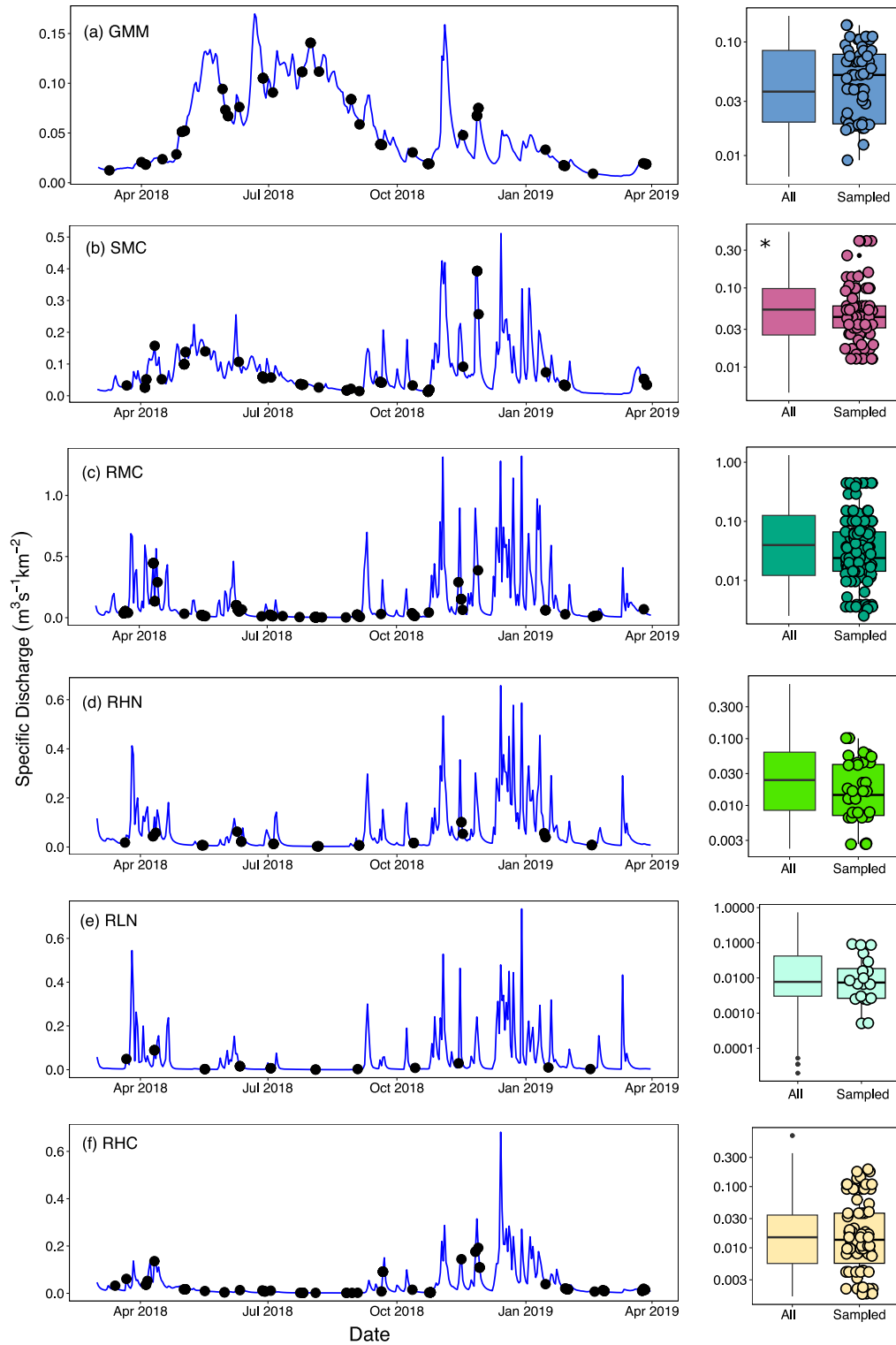
Figure 2. Streamflow conditions during the study period and during sampling events, with each row representing a different watershed type. Stream hydrographs are shown in blue with an overlay of sampled flows shown as black dots. Boxplots compare the distribution of sampled flows and observed flows on a log-transformed scale. The log transformation emphasizes the variation between low and moderate flows, which was well captured by the samples. An asterisk (*) indicates where the two distributions were significantly different at the 0.05 level based on a two-sample Kolmogorov–Smirnov test performed on untransformed flow values. Phase 1 dataset.

GMM and SMC types. Meltwater freshet continued through the summer months in the GMM type. Rain types had sustained low flow periods (< 0.01 $m^3 s^{-1} km^{-2}$) in summer and many short duration high flow events (> 0.1 $m^3 s^{-1} km^{-2}$) in fall and winter. Sampling events were well distributed across the hydrograph in each watershed type (Figure 2). Although extremely high flows (> 0.5 $m^3 s^{-1} km^{-2}$) were not captured, samples were collected across all seasons and a wide range of flow conditions (0.0005 $m^3 s^{-1} km^{-2}$ to 0.446 $m^3 s^{-1} km^{-2}$). The distribution of sampled flows was not significantly different from the distribution of all flows ($p < 0.05$) for any watershed type except the Snow Mountains (SMC) type. In the SMC type, the median flow of our sample (0.043 $m^3 s^{-1} km^{-2}$) was somewhat (0.010 $m^3 s^{-1} km^{-2}$ or $\sim 19\%$) lower than the median flow of the study period (0.053 $m^3 s^{-1} km^{-2}$) and we missed the extremes (high and low).

Table 2. A Summary of the Proportion of Variance Explained and Component Loadings of the Original Descriptors for the First Three Principal Components (PC) of Stream Biogeochemistry, Based on an Analysis of 184 Samples Collected (without missing values) From the $n = 56$ Sampled Watersheds (Phase 1 dataset)

	PC1	PC2	PC3
Proportion of variance	0.47	0.18	0.09
Cumulative proportion	0.47	0.65	0.74
DOC	− 0.87	0.3	− 0.01
DON	− 0.66	0.46	− 0.09
DIN	0.71	0.08	0.19
TP	0.48	0.18	− 0.78
DOP	0.30	0.20	− 0.77
SRP	0.42	0.56	− 0.2
SiO2	0.91	0.28	0.1
EC	0.62	0.68	0.18
pH	0.86	0.00	0.03
Temp	− 0.07	0.27	− 0.34
Fe	− 0.73	0.28	− 0.36
Na	− 0.08	0.91	0.20
Ca	0.85	0.27	0.06
Mg	0.36	0.86	0.10
K	0.77	0.12	− 0.15
Al	− 0.82	0.04	− 0.28
Alk	0.92	0.10	0.14
O18	− 0.75	0.49	0.17
H2	− 0.76	0.47	0.21
Na:Ca	− 0.81	0.29	0.07

Water Quality Gradients Across Small Coastal Watersheds

The first two principal components of a PCA of freshwater data explained 65% of the total variance in the original 20 properties (Table 2, Figure 3). Increasing PC1 (47% of observed variance) described decreasing concentrations of organic matter associated variables (DOC, DON, Fe, and Al^{3+}; increasing pH) and increasing DIN concentrations. Increasing PC1 also described decreasing Na:Ca, decreasing $\delta^{18}O$-H_2O and δ^2H-H_2O, and increasing concentrations of several variables associated with chemical weathering of rocks (SiO_2, Alkalinity, Ca^{2+}, and K^+). This component reflected a high degree of statistically significant association among subsets of the water quality variables (Supplemental Text S2; Figure S5). Mean PC1 scores differed significantly ($p < 0.001$) across watershed types (Table 3), with high scores in Glacierized type watersheds and low scores in three Rain type watersheds (RLN, RHN, RMC; Figure 3b). PC2 (18% of observed variance) primarily described increasing concentrations of Na^+ and Mg^{2+} (Table 2). Mean PC2 scores also differed significantly ($p < 0.001$) across watershed types (Table 3), with high scores in the Rain Lowlands and low scores in the Mountains types (Figure 3c and Figure S6). The broad spatial patterns of riverine water quality associated with PC1 were not sensitive to the methodological choice to either include all time points from all watersheds (as done in Figure 3) or to examine the average biogeochemistry of watersheds with larger sample sizes ($n \geq 3$) and more similar lithology (as done in Figure S6).

Typical Riverine Water Quality of each Watershed Type

In addition to differences in PC scores, we found that 20 of the 22 water quality properties were significantly different across watershed types (Table 3). This included differences in chemistry associated with dissolved organic matter, inorganic nutrients, chemical rock weathering products, and water related isotopes. Only temperature ($p = 0.157$) and turbidity ($p = 0.055$) were not significantly different across types, reflecting similarities between specific types (for example, RHC and RLN) and variability within types (for example, RLN temperature). Despite this, mean temperature clearly decreased and turbidity clearly increased along the broader topo-climatic gradient from Rain to Glacierized type watersheds (Table 3).
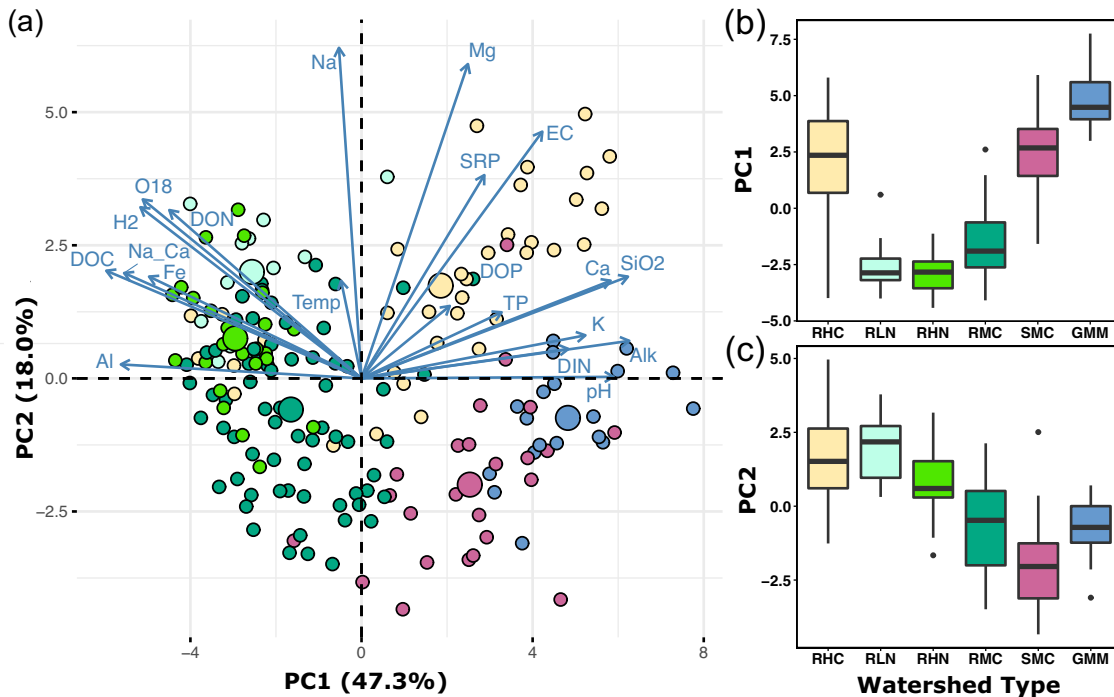
Figure 3. Ordination biplot **a** showing the first two principal components of river biogeochemistry data (20 variables), colored by watershed type. Each small point represents one of $n = 184$ samples collected (without missing values) from the $n = 56$ sampled watersheds. Large points represent group mean coordinates. Watershed types are defined in Figure 1. Boxplots in **b** and **c** show the distribution of PC scores all 184 observations, grouped by watershed type. Phase 1 dataset.

Water quality properties that were associated with organic matter were particularly variable over the gradient of watershed types. DOC, DON, Fe, and Al^{3+} generally increased in concentration from Glacierized Mountains type watersheds (mean ± standard error: 1.2 ± 0.1 mg L^{-1} DOC, 30.4 ± 4.6 µg L^{-1} DON, 67.3 ± 20.3 µg L^{-1} Fe, 77.7 ± 24.7 µg L^{-1} Al^{3+}) to Rain Lowlands type watersheds (15.1 ± 1.0 mg L^{-1} DOC, 215.6 ± 20.4 µg L^{-1} DON, 441.0 ± 77.7 µg L^{-1} Fe, 312.0 ± 13.9 µg L^{-1} Al^{3+}) (Table 3). Among the Rain type watersheds on the Rivers Inlet transect, these organic matter associated properties increased (and pH decreased) along a topographic sequence from Mountain, to Hill, to Lowland types.

Most of the nitrogen in these rivers occurred in dissolved form (Figure 4a). Dissolved nitrogen was predominantly organic (DON) in the Rain type watersheds (Figure 4c), with mean DON between two and seven times higher in the Rain watershed types (82.8 ± 9.5 µg L^{-1} in RMC to 215.6 ± 20.4 µg L^{-1} in RLN) than the Snow (28.5 ± 4.6 µg L^{-1}) and Glacierized (30.4 ± 4.6 µg L^{-1}) types, broadly tracking the pattern of DOC across watershed types (Table 3). Mean DIN and the % DIN (of TDN) were highest in the GMM type (85.2 ± 15.2 µg L^{-1} DIN) and generally increased

along the topographic gradient from Lowland (11.9 ± 2.2 µg L^{-1} DIN) to Mountain watershed types (Figure 4c; Table 3). The RHC watershed type was an exception to this pattern, with the second highest mean DIN (68.5 ± 15.1 µg L^{-1}), yet only Hill-type relief (Table 3).

The majority of the phosphorous in these rivers occurred in dissolved form, except that particulate phosphorous was typically dominant in the GMM type (Figure 4b; Table 3). The dissolved phosphorous was predominantly organic (DOP) in all watershed types and this proportion did not vary appreciably by watershed type (Figure 4d). Mean SRP was low in all watershed types (≤ 2.0 µg L^{-1}), reaching highest mean concentrations in the RHC type (2.0 ± 0.6 µg L^{-1}; Table 3).

The seasonality of riverine water quality also varied with watershed type (Figure 5). In the Glacierized watershed type, median turbidity and PP concentrations during the meltwater season (May to September; 8.8 FNU and 15.5 µg L^{-1}, respectively) were four to five times higher than during the rain-driven season (2.1 FNU and 3.0 µg L^{-1}, respectively) and at least five times higher than any other watershed type (up to 1.2 FNU and 3.0 µg L^{-1}, respectively) during the meltwater season (Figure 5a, b). Median May to September

Table 3. Mean (in bold), Standard Error (se), Number of Watersheds (n), and Statistical Test Results for Three Principal Components and 22 River Biogeochemistry Measurements Grouped by Watershed Type

Descriptor	RHC Mean	se	n	RLN Mean	se	n	RHN Mean	se	n	RMC Mean	se	n	SMC Mean	se	n	GMM Mean	se	n	p
PC1	**1.2**	1.1	6	**− 3.6**	0.5	4	**− 3.7**	0.5	4	**− 1.6**	0.4	15	**3.2**	0.7	15	**5.0**	0.4	8	< 0.001
PC2	**1.8**	0.8	6	**2.7**	0.4	4	**0.4**	0.5	4	**− 1.2**	0.4	15	**− 1.0**	0.2	15	**0.9**	1.0	8	< 0.001
PC3	**0.6**	0.4	6	**− 0.1**	0.2	4	**0.2**	0.3	4	**0.3**	0.2	15	**− 0.9**	0.6	15	**− 0.3**	0.6	8	0.135
DOC (mg L^{-1})	**5.4**	1.9	6	**15.1**	1.0	4	**9.3**	1.6	4	**6.4**	0.8	16	**1.9**	0.3	16	**1.2**	0.1	9	< 0.001
DON (µg L^{-1})	**96.0**	22.2	6	**215.6**	20.4	4	**135.8**	21.0	4	**82.8**	9.5	16	**28.5**	4.6	16	**30.4**	4.6	8	< 0.001
DIN (µg N L^{-1})	**68.5**	15.1	6	**11.9**	2.2	4	**15.9**	2.7	4	**39.6**	6.6	16	**56.9**	12.0	16	**85.2**	15.2	9	0.001
TP (µg L^{-1})	**15.0**	2.3	6	**10.1**	1.2	4	**6.4**	0.5	4	**6.6**	0.9	16	**14.5**	0.8	16	**40.9**	15.8	9	< 0.001
DOP (µg L^{-1})	**8.8**	1.6	6	**4.5**	0.3	4	**3.8**	0.5	4	**4.2**	0.9	15	**11.8**	1.3	15	**10.3**	2.1	9	< 0.001
SRP (µg L^{-1})	**2.0**	0.6	6	**1.6**	0.2	4	**0.8**	0.1	4	**0.8**	0.1	16	**1.3**	0.2	16	**1.7**	0.6	9	0.019
SiO$_2$ (µg Si L^{-1})	**1,164.7**	481.7	6	**119.3**	75.2	4	**43.5**	14.7	4	**116.4**	42.1	16	**526.6**	146.5	16	**955.6**	48.4	9	< 0.001
EC (µS cm^{-1})	**32.7**	7.6	6	**26.6**	3.5	4	**18.5**	2.1	4	**13.1**	1.1	16	**17.8**	3.1	16	**32.7**	2.3	9	< 0.001
pH	**6.5**	0.4	6	**4.8**	0.2	4	**5.0**	0.3	4	**5.5**	0.2	16	**6.8**	0.1	16	**7.1**	0.1	9	< 0.001
Temp (°C)	**9.8**	0.6	6	**9.7**	1.8	4	**10.5**	0.9	4	**8.5**	0.5	16	**8.3**	0.5	16	**7.7**	0.4	9	0.157
Fe (µg L^{-1})	**93.3**	36.5	6	**441.0**	77.7	4	**245.4**	40.0	4	**170.9**	27.8	16	**41.4**	7.3	16	**67.3**	20.3	9	< 0.001
Na (µg L^{-1})	**2,069**	339	6	**3,006**	426	4	**1,982**	191	4	**1,203**	113	16	**756**	119	16	**1,051**	203	9	< 0.001
Ca (µg L^{-1})	**3,871**	1148	6	**1,507**	474	4	**719**	161	4	**1,186**	190	16	**2,955**	486	16	**4,917**	601	9	< 0.001
Mg (µg L^{-1})	**459.3**	90.2	6	**457.8**	52.8	4	**305.1**	24.8	4	**244.6**	20.4	16	**226.1**	23.5	16	**355.0**	77.8	9	0.002
K (µg L^{-1})	**226.6**	81.5	6	**161.9**	12.4	4	**140.0**	14.1	4	**156.3**	14.1	16	**429.5**	98.3	16	**756.2**	53.9	9	< 0.001
Al (µg L^{-1})	**132.6**	52.2	6	**310.2**	13.9	4	**234.2**	32.4	4	**192.3**	19.5	16	**84.5**	15.3	16	**77.7**	24.7	9	< 0.001
Alk (mg CaCO$_3$ L^{-1})	**9.9**	3.3	6	**1.5**	0.8	4	**0.8**	0.3	4	**2.0**	0.6	16	**5.1**	1.1	16	**10.5**	1.6	9	< 0.001
δ^{18}O-H$_2$O (‰)	**− 11.9**	0.3	6	**− 9.8**	0.2	4	**− 9.4**	0.3	4	**− 11.5**	0.2	16	**− 14.6**	0.2	16	**− 16.5**	0.5	9	< 0.001
δ^2H-H$_2$O (‰)	**− 86.5**	2.2	6	**− 70.7**	0.7	4	**− 69.1**	1.5	4	**− 82.3**	1.8	16	**− 106.6**	1.8	16	**− 121.2**	4.0	9	< 0.001
Na:Ca (mass)	**0.9**	0.3	6	**4.8**	1.9	4	**3.3**	0.7	4	**1.5**	0.2	16	**0.4**	0.1	16	**0.2**	0.0	9	< 0.001
Turbidity (FNU)	**3.4**	2.4	6	NA	NA	0	**2.1**	0.6	3	**0.4**	0.1	8	**5.2**	1.5	8	**13.5**	6.6	9	0.055
PP (µg L^{-1})	**4.8**	1.4	6	**4.4**	1.0	4	**1.9**	0.2	4	**2.3**	0.3	15	**4.4**	0.8	15	**30.3**	14.3	9	0.002

Watershed types are defined in Figure 1. The p-values (p) reflect one-way ANOVA tests for equal means. Phase 2 dataset.
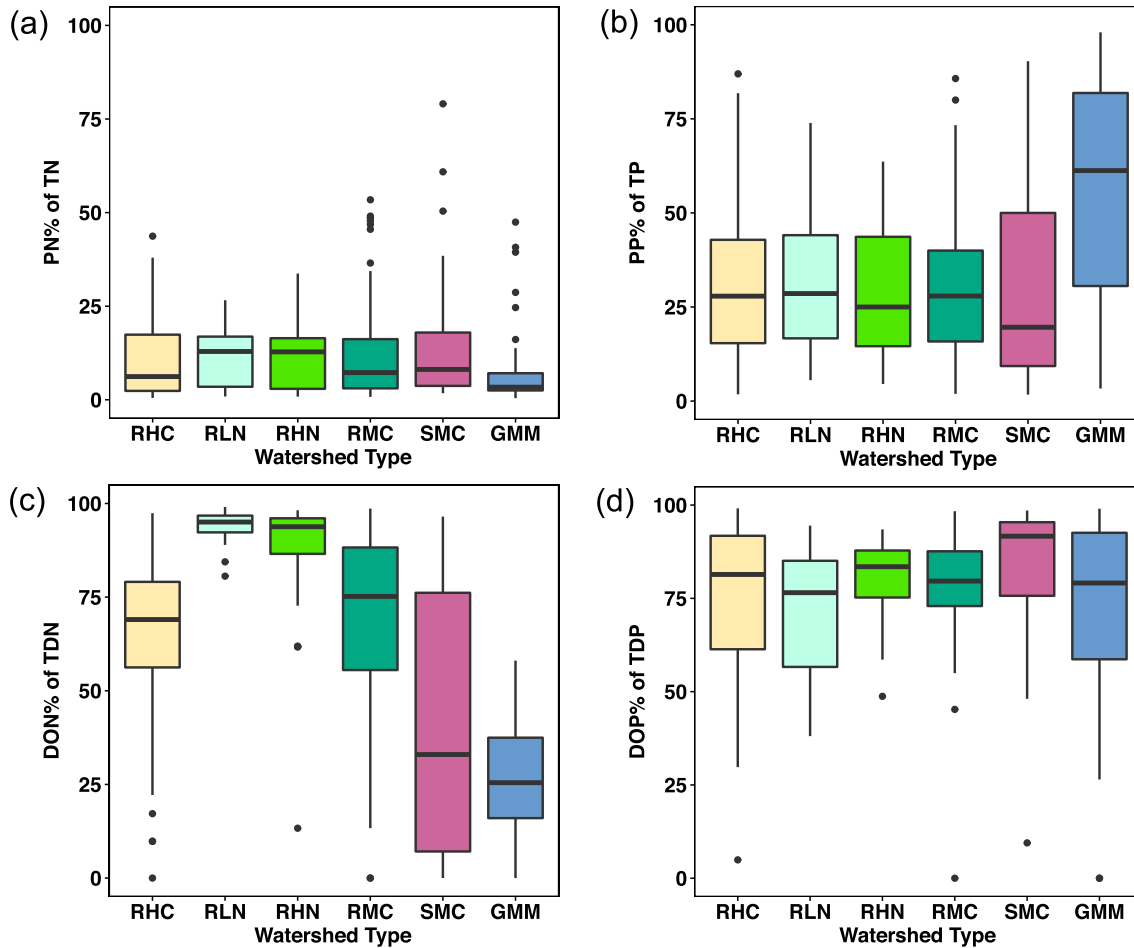
Figure 4. Boxplots showing the proportion of N (**a**) and P (**b**) in particulate form and the proportion of dissolved N (**c**) and P (**d**) in organic form, across watershed types. Phase 2 dataset.

water temperature decreased ~ 6 °C along the gradient from Rain (~ 14—11 °C), to Snow (~ 10 °C), to Glacierized (~ 8 °C) watershed types, with a corresponding decrease in the seasonal range of temperatures from ~ 8 °C in the RHC type to ~ 2 °C in the GMM type (Figure 5c). Season had a comparatively subtle influence on specific conductance (EC) in most watershed types (Figure 5d). In the GMM and SMC watershed types, median EC was slightly (between ~ 7 and ~ 4 µS cm^{-1}) lower in the meltwater season. In the RHC watersheds by contrast, median EC was highest in the May to September period at ~ 44 µS cm^{-1}, nearly double the rain-driven season EC (~ 23 µS cm^{-1}).

Catchment Controls on Riverine Water Quality

We evaluated the performance of several alternative water quality models as a means of inferring the relative importance of different groups of pre-

dictors (Table 4). Based on random forest regression, watershed type explained much of the water quality variation observed among watersheds (Table 4). Watershed type alone explained 67% and 58% of the total variation in PC1 (which indicated a gradient from concentrated organics to concentrated rock weathering products) and DOC, respectively. Using the 12 classification variables as predictors substantially increased the percentage of total variance explained for all water quality-related response variables. This finding indicates that some of the water quality variation between watersheds of the same type was explained by the characteristics of individual watersheds (for example, maximum watershed elevation). Adding watershed type, lithology, seral stage, non-forest cover, and waterbody cover as additional predictors did not meaningfully improve the model for any response variable, except for a very small (2.3%) increase in the variance explained for PC2. Despite this, seral stage variables ranked as important pre-
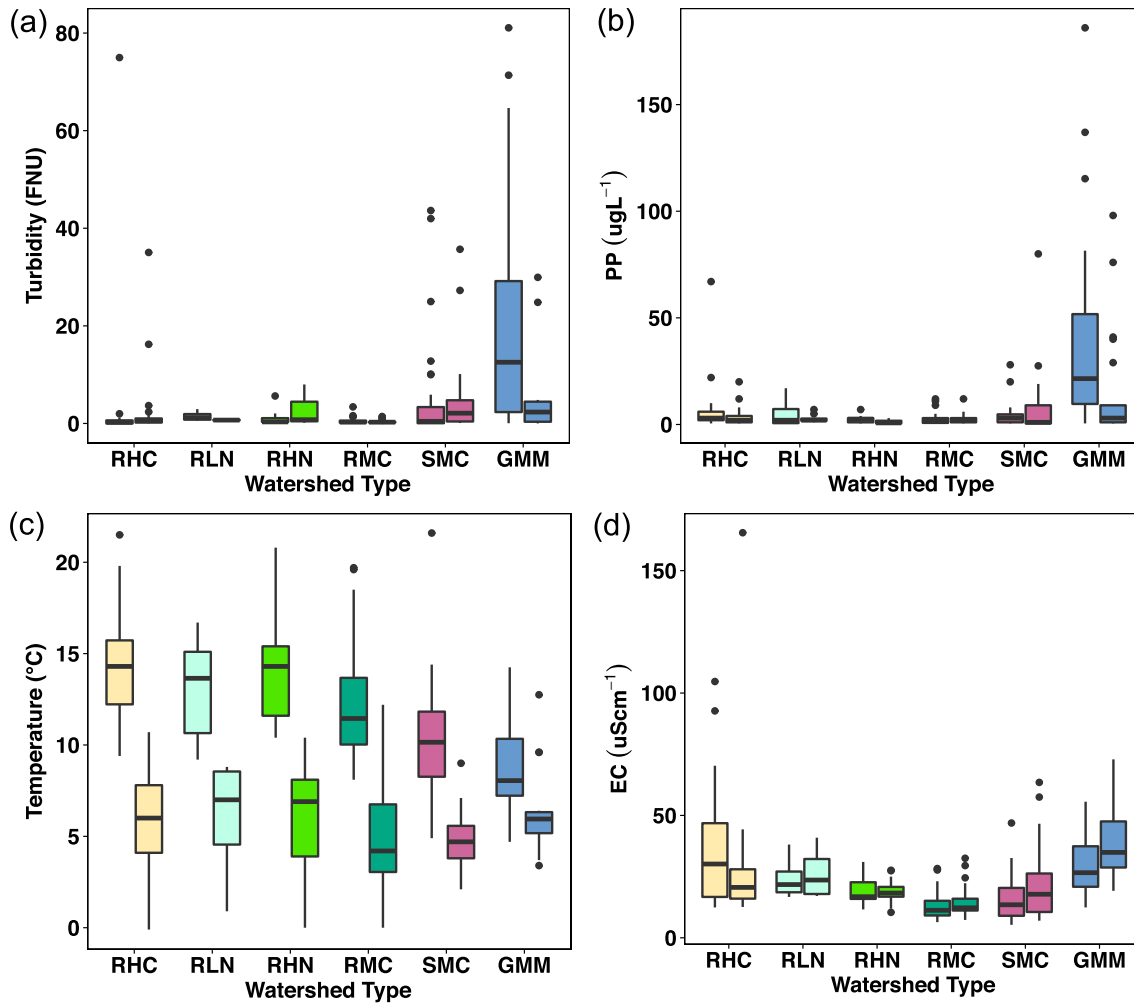
Figure 5. Boxplots showing turbidity **a**, PP concentrations **b**, temperature **c**, and EC **d** across watershed types and seasons. The first (left) boxplot in each watershed type shows the meltwater (May to September) season and the second (right) shows the rain (October to April) season. Phase 2 dataset, using individual sample days rather than watershed average values

Table 4. Estimated Percentage of Water Quality Variance Explained by Random Forest Modeling Using Alternative Sets of Watershed Characteristics as Predictor Variables

Response	n	Watershed type		12 metrics		Lithology		Seral stage		All variables	
		RMSE	VE (%)	RMSE	VE (%)	RMSE	VE (%)	RMSE	VE (%)	RMSE	VE (%)
PC1	41	1.9	66.6	1.2	86.8	3.1	12.3	2.7	30.9	1.2	87.2
PC2	41	1.6	34.8	1.3	58.1	1.8	12.1	1.8	20.4	1.2	60.4
DOC	45	3.0	58.1	1.9	83.9	4.0	23.8	3.8	32.9	1.9	83.4
SiO_2	45	532.4	23.2	467.9	40.7	589.8	5.7	516.3	27.7	482.9	36.8
Alk	45	4.3	30.8	3.6	51.2	4.8	11.7	4.1	37.0	3.7	47.1
Turbidity	32	8.5	− 2.4	6.8	35.7	7.7	16.6	8.6	− 4.5	6.8	35.5

The 12 metrics model used the watershed classification variables (for example, maximum elevation and mean annual temperature) as predictors. The lithology model used the proportional cover of the nine lithologic classes as predictors. The seral stage model used the proportion of the forest area in the four seral stages as predictors. The all variables model used non-forest cover and water body cover in addition to all variables included in earlier models: watershed type, 12 metrics, lithology, and seral stage. RMSE = root mean squared error; VE = % variance explained. Phase 2 dataset.
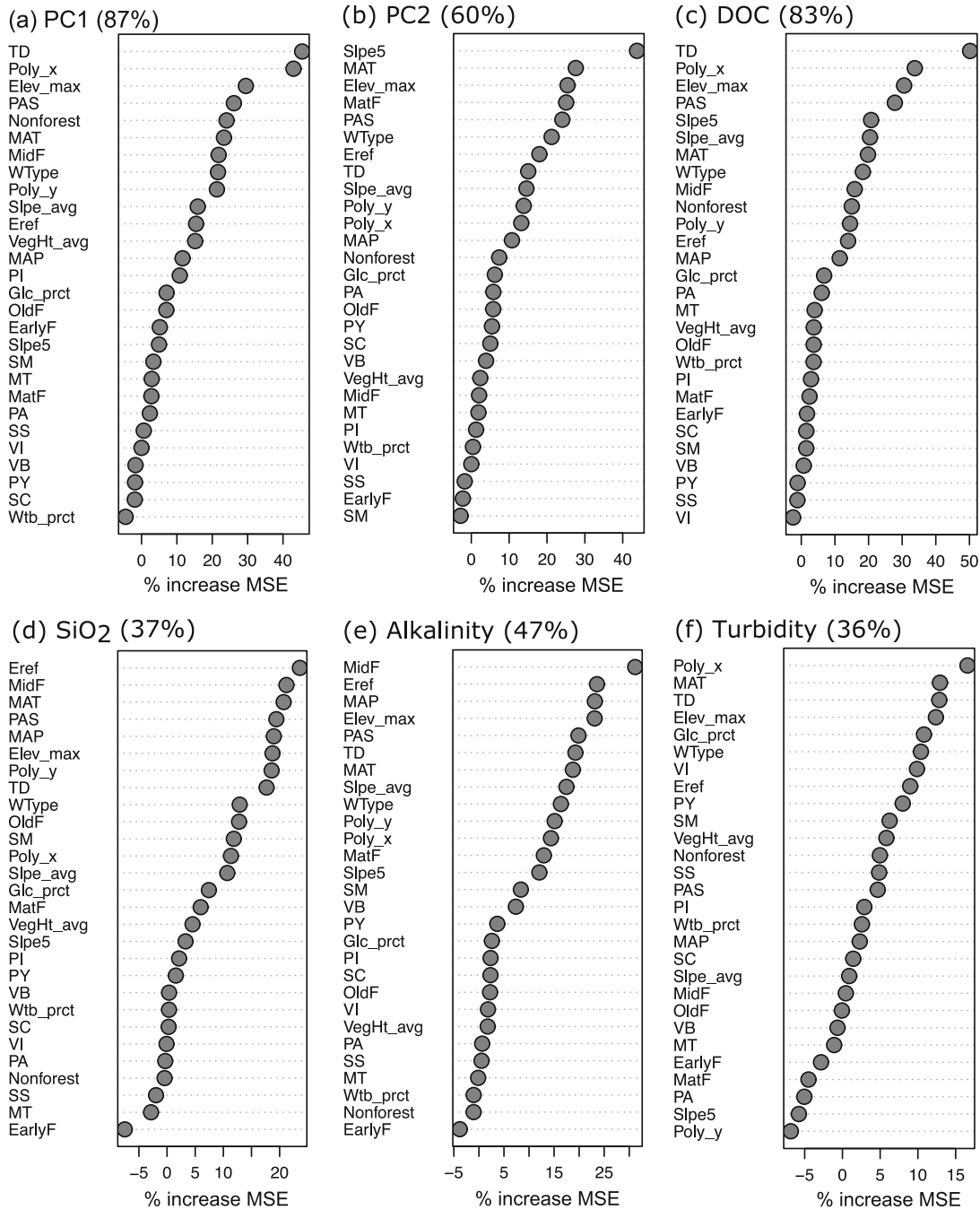
Figure 6. Random forest variable importance plots for prediction of six water quality response variables from the suite of all candidate predictor variables. Predictor variables include watershed type (WType), the 12 metrics used to define watershed type (Table 1), all nine lithology variables (Table S1), and all five forest cover variables: early-seral forest (EarlyF), mid-seral (MidF), mature forest (MatF), old forest (OldF), and non-forest (Nonforest). Sample sizes were 41 for PC1 and PC2, 45 for DOC, SiO$_2$, and alkalinity, and 32 for turbidity. Phase 2 dataset.

dictors for some of the water quality variables (Figure 6) indicating potential confounding of forestry disturbance with other watershed characteristics such as latitude and precipitation (Figure S3). Of these 12 characteristics that defined the watershed types, the three most important predictors for PC1 and DOC were TD (continentality; see Table 1 for variable definitions), Poly_x (∼ longitude), and Elev_max (relief) (Figure 6a, c). No combination of watershed characteristics explained more than 51% of the spatial variation in SiO$_2$, alkalinity, or turbidity with random forest models (Table 4).
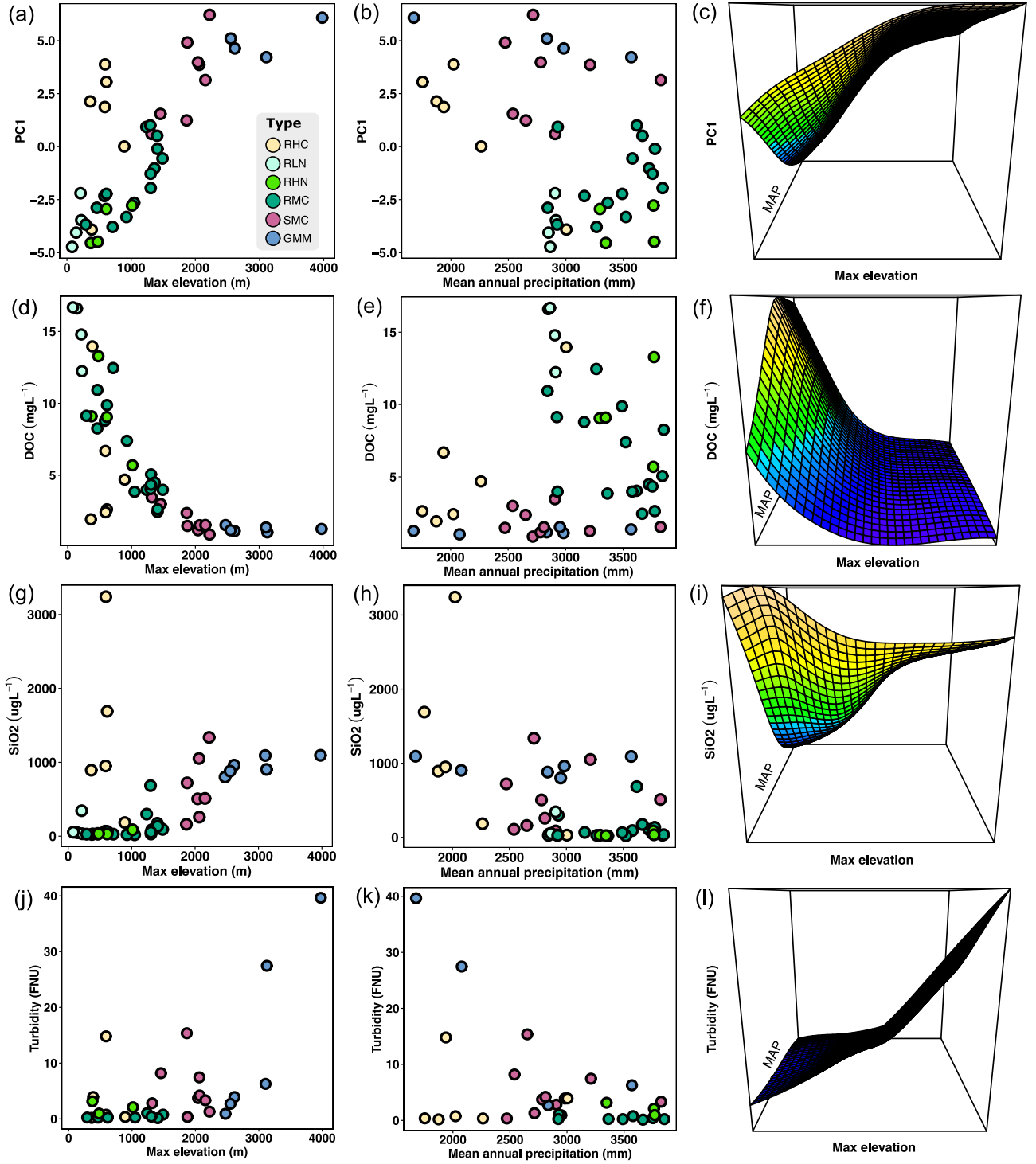
Figure 7. Spatial controls on mean streamflow biogeochemistry of individual watersheds. This figure shows the bi-variate scatterplots (first and second columns) and a nonlinear smoothing function (GAM) (third column) used to visualize how watershed elevation and precipitation interact to predict PC1 and three representative chemistry variables. Watersheds are color coded by type as per Figure 1. The GAM models based on the interaction of elevation and MAP had adjusted R^2 values of 0.91 for PC1 ($p < 0.001$, $n = 41$), 0.87 for DOC ($p < 0.001$, $n = 45$), 0.53 for SiO$_2$ ($p < 0.001$, $n = 45$), and 0.75 for turbidity ($p < 0.001$, $n = 32$). Phase 2 dataset.

Comparison of watershed types suggested that topography and climate were important and potentially interacting controls on riverine water quality. To better visualize these potential interacting effects at the watershed scale of analysis, we specified a simple two-variable interaction model with mean annual precipitation (MAP) and a representative topographic variable (Figure 7). We selected maximum elevation (relief) as the representative topographic variable because it was the best topographic predictor of PC1 and an important predictor of PC2, DOC, SiO_2, alkalinity, and turbidity (Figure 6). Most (91%) of the variation in PC1 was explained by the interaction of relief and precipitation ($R^2 = 0.91$, $p < 0.001$; Figure 7c). PC1 scores were lowest in low-elevation watersheds with high precipitation and increased with increasing elevation or decreasing precipitation. DOC showed the opposite pattern, peaking in wet, low-elevation watersheds and declining exponentially with elevation and with decreasing MAP ($R^2 = 0.87$, $p < 0.001$; Figure 7f).

In contrast with DOC, SiO_2 concentrations were high in both drier, low relief watersheds and in high-relief watersheds, with very low concentrations in the wet, lowland watersheds (Figure 7i). However, only about half of the variation in SiO_2 was explained by the interaction of relief and precipitation ($R^2 = 0.53$, $p < 0.001$) indicating that some important controlling mechanism was not represented by this model. Turbidity was well explained by this model ($R^2 = 0.75$, $p < 0.001$), which predicted an abrupt increase from moderate- to high-relief watersheds.

The strong predictive link between maximum watershed elevation and riverine water quality likely reflected the effects of multiple controlling factors. Maximum watershed elevation was correlated with increasing watershed slope ($r = 0.7$), precipitation as snow ($r = 0.9$), continentality ($r = 0.7$), glacier cover ($r = 0.7$), and watershed area ($r = 0.6$) as well as decreasing mean annual temperature ($r = -1$) and vegetation height ($r = -0.7$) (Figure S3). In fact, continentality (TD) was the most important predictor of PC1 (Figure 6). Watershed glacier cover was largely absent from watersheds below 2,000 m and then rose rapidly above this elevation, leading to a nonlinear association with watershed elevation (Figure S3c). Furthermore, while the low-elevation watersheds were almost exclusively acid plutonic bedrock, the high-elevation watersheds had more diverse lithologies with only $\sim$ 50–75% acid plutonic bedrock (Table S1) and some sedimentary rock cover (Figure S3d). Forest seral stages showed no

correlation with maximum watershed elevation but mid-seral ($r = -0.5$) and old forest ($r = 0.5$) cover were both moderately correlated with MAP (Figure S3).

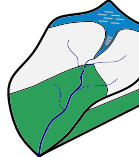## Magnitude of Freshwater Export by Watershed Type

We estimated the extent and discharge of each watershed type between the northern and southern extent of our field study as a means of describing the magnitude of riverine exports from each type (Table S3). The 18 glacierized watersheds (of 1,989 in total) represented 50% of the total drainage area and contributed $\sim$ 44% of total freshwater discharge, reflecting their large average size (1,168 km^2). Despite very small average size (6 km^2), Rain type watersheds contributed a third (33%) of discharge, because they were numerous (1,705 watersheds) and had high specific discharge on average. Rain Mountain type watersheds (RMC) accounted for 26% of discharge and only 15% of the drainage area, reflecting a very high specific discharge. A much smaller number of Snow type watersheds (266) contributed the remaining 23% of cumulative discharge.

DISCUSSION

Spatial Heterogeneity of Small Coastal Watershed Ecosystems

Meso-scale mapping and classification of small coastal watersheds revealed a high degree of spatial heterogeneity in watershed characteristics. The two fjordland systems we studied spanned from some of the most glacierized coastal watersheds in BC, to the most wetland-dominated watershed type in the NPCTR, to a drier type of watershed found as far south as Oregon (Giesbrecht and others 2022). These findings show how the physiographic complexity of a coastal margin can translate to intense spatial gradients of watershed-scale topography, climate, glaciers, and terrestrial ecosystems. As a consequence, a substantial range of the watershed diversity previously described at a regional scale in the NPCTR was represented in just two fjordland complexes.

Riverine water quality also varied dramatically over short distances in association with spatial variation in watershed characteristics (Figure 8). For example, the range of watershed-averaged DOC concentrations observed across the $< 2°$ latitude in this study (0.87 to 16.69 mg L^{-1}) represented nearly the full range of the DOC

	Rain Hills - Central	Rain Lowlands	Rain Hills - Northern	Rain Mountains	Snow Mountains	Glacierized Mountains
Watershed controls	• Rainshadow climate • Low-mod. relief • Productive forest • Deep/mineral flowpaths • Forest disturbance	• Hypermaritime climate • Low relief • Bog forest • Shallow flowpaths • Marine salt inputs	• Hypermaritime climate • Low-mod. relief • Bog forest • Shallow flowpaths • Marine salt inputs	• Transitional climate • Mod. relief • Productive forest • Shallow flowpaths	• Cold and snowy climate • High relief • Deep/mineral flowpaths • Forest disturbance	• Very cold and snowy • Glacial processes • Very high relief • Deep/mineral flowpaths • Some sedimentary rock • Forest disturbance
Water quality	• Clear/humic stained • Highest summer temps • Mod. DOM+ • High inorganic nutrients • High weathering solutes • High buffering, mod. pH	• Humic stained • Highest summer temps • Very high DOM+ • Low inorganic nutrients • Low weathering solutes • Low buffering and pH	• Humic stained • Highest summer temps • High DOM+ • Low inorganic nutrients • Low weathering solutes • Low buffering and pH	• Clear/humic stained • Mod. summer temps • Mod. DOM+ • Mod. inorganic nutrients • Low weathering solutes • Low buffering and pH	• Clear • Cool summer temps • Low DOM+ • High inorganic nutrients • Mod. weathering solutes • Mod. buffering, high pH	• Seasonally turbid • Coolest summer temps • Low DOM+ • High inorganic nutrients • High weathering solutes • High buffering and pH

Figure 8. Integrative conceptual summary of watershed controls on riverine water quality across six watershed types in the NPCTR, for watersheds dominated by plutonic-metamorphic lithology. Terms like ''low'' and ''high'' are used to rank the watershed types relative to other watershed types in this study area rather than make a global comparison. For example, our ''high inorganic nutrients'' are not high in a global context. ''DOM + '' refers to DOM-associated properties: high DOC, high DON, high Fe, high Al, and low pH. Additional potential controls are discussed in the main text, including watershed size, trace carbonate rock, anadromous fish, and atmospheric deposition.

concentration observations from watershed outlets across the $> 20°$ latitude of the entire NPCTR region (0.57 to 12.49 mg L^{-1}; Giesbrecht and others 2022). The case of DON further illustrates the wide range of organic matter concentrations over a relatively short distance. The RLN and RHN type watersheds had much higher DON (215.6 ± 20.4 µg L^{-1} and 135.8 ± 21.0 µg L^{-1}, respectively) than typical of small unpolluted streams of the temperate region (56 to 61 µg L^{-1}; Meybeck 1982) or very small (< 1 km^2) temperate forested watersheds of Chile and Argentina (8 to 135 µg L^{-1}; Perakis and Hedin 2007). However, even the RLN and RHN type watersheds in our study had much lower DON than typical of contaminated rivers globally (416 to 1490 µgL^{-1}; Meybeck 1982), reflecting the absence of major agricultural land use or point source pollution in this study area. In contrast with the RLN and RHN types, rivers draining the Snow and Glacierized Mountain type watersheds in our study had very low DON (28.5 ± 4.6 µg L^{-1} to 30.4 ± 4.6 µg L^{-1}) compared to typical forested watersheds around the world (Meybeck 1982; Perakis and Hedin 2007). Over the relatively small geographic range of our study, we also observed a switch from predominantly organic forms of dissolved nitrogen in Rain type watersheds—which is typical of unpolluted temperate rainforest streams (Perakis and Hedin 2002)—to predominantly inorganic forms in Snow and Glacierized type watersheds. Furthermore, we observed a switch from predominantly particulate forms of phosphorous in the Glacierized Mountain watershed type to predominantly dissolved organic forms in all other watershed types, presumably reflecting a shift from physical to biological process controls on phosphorous budgets as glacier cover decreases (Filippelli and others 2006; Moore and others 2009; Milner and others 2007).

The previously defined watershed types (Giesbrecht and others 2022) captured a meaningful amount of spatial variation in many aspects of riverine water quality (Figure 8). As such, watershed classification in the NPCTR can be used to distinguish not only streamflow regimes and DOC dynamics (Giesbrecht and others 2022) but also broad aspects of riverine water quality (for example, DON, Fe, and pH). Specifically, the multivariable water quality description we developed for each watershed type (Table 3) offers a first approximation of the average riverine water quality in unsampled areas with similar watershed characteristics. However, catchment-specific watershed characteristics can be used for improved prediction in unsampled watersheds (Table 4; Figure 7). In particular, maximum watershed elevation appears to serve as a surrogate measure of multiple spatial controls on riverine water quality, particularly after accounting for the interaction with regional climatic gradients such as the rainshadow effect of Vancouver Island. Our findings suggest that easily calculated topo-climatic watershed characteristics are useful for predicting water quality in unsampled watersheds of rainforest fjordlands (Supplemental Information, Text S3). More accurate predictive modeling would require

accounting for temporal controls (for example, seasons, storms, and snowmelt) and additional spatial controls (for example, lithology and forest cover), particularly for certain response variables such as turbidity, alkalinity, and SiO_2.

Spatial Controls on Water Quality Patterns in the Rainforest

Our study was designed to sample the extant range of watershed characteristics in our study area rather than isolate individual controlling factors, yet we discuss some potential spatial controls underlying the patterns we observed. The associations between water quality and watershed characteristics in this study are consistent with the hypothesis that climate and topography are the dominant controls on many aspects of riverine water quality at the coastal margin of these rainforest fjordlands (Figure 8). For example, watersheds with low-to-moderate relief and a very rainy climate (RHN, RLN) had high concentrations of DOM-associated solutes (DOC, DON, Fe, and Al^{3+}) and low concentrations of inorganic nutrients (DIN, SiO_2, SRP). This extremely DOM-dominated water quality regime is probably a function of a wet hypermaritime climate (Giesbrecht and others 2022; Perakis and Hedin 2007), organic matter accumulation on gently sloping lowland topography (Oliver and others 2017; McNicol and others 2019), shallow flowpaths through organic-rich wetlands and hillslopes (D'Amore and others 2015; Fitzgerald and others 2003; Fellman and others 2009; Gibson and others 2000), and relatively passive transport of DOM through small watersheds (Raymond and others 2016). Conversely, denitrification in wetland soils (Schlesinger 1997) could partly explain the low stream DIN concentrations in these watersheds. These watershed types also had the highest $\delta^{18}O\text{-}H_2O$ and $\delta^2H\text{-}H_2O$, likely reflecting very close proximity to the ocean and the relatively limited amount of precipitation that can occur before air masses from the Pacific ocean encounter these watersheds (Drever 1982).

At the other topo-climatic extreme, our Glacierized Mountains watershed type had many—but not all—of the water quality characteristics found in glacierized watersheds of the NPCTR in Southeast Alaska (Fellman and others 2014a, b; Hood and Berner 2009; Milner and others 2017). For example, compared to other watershed types, the GMM type had water quality signatures indicative of more rapid erosion and weathering of bedrock, slower production of DOM, dilution of DOM, and thermal buffering by elevation, snow, and ice

(Figure 8). Our water quality samples were collected far downstream of the glaciers themselves and likely reflected both the direct and indirect influence of glaciers and other correlated watershed characteristics such as elevation, slope, and non-forest cover. Deeper flowpaths on steep slopes and in valley bottom alluvium likely also contributed to the low concentrations of DOM and higher concentrations of rock weathering products (Covino and others 2007; Laudon and Sponseller 2018). In contrast with studies in Southeast Alaska (Hood and Berner 2009; Milner and others 2017), further south in the NPCTR we found that glacierized watersheds had elevated riverine DIN similar to findings in Europe (for example, Colombo and others 2019) and the US Rocky Mountains (for example, Slemmons and others 2013; Ren and others 2019). The sources of elevated DIN in glacier runoff remain unclear but likely include combinations of rock weathering and atmospheric deposition (Slemmons and others 2017), the latter of which increases down the NPCTR coast from Southeast Alaska through BC (Hember 2018). Nitrogen fixation in recently deglaciated areas (Milner and others 2007) and the forested portion of the lower watershed may have also played a role in shaping riverine water quality at the coastal outlet in our study area.

This study suggests that a rainshadow climate can have a major effect on the spatial pattern of riverine water quality within a rainforest region, independent of watershed topography, highlighting a largely unexplored physiographic control on aquatic biogeochemistry at the land–sea margin. Specifically, watersheds in the rainshadow of Vancouver Island (RHC type) had notably different water quality compared to topographically similar watersheds (RHN type) outside the rainshadow: lower concentrations of DOM-associated solutes, higher DIN, lower DON % of TDN, higher SiO_2, and higher pH and buffering due to more concentrated products of chemical rock weathering. The distinct water quality regime observed in these drier and warmer conditions (for example, precipitation minus evaporation $\sim 1{,}431$ mm in RHC vs. $\sim 3{,}033$ mm in RHN) is expected to be promoted by less soil organic matter accumulation at the surface and more DOM adsorption on mineral particles (McDowell and Wood 1984; Perakis and Hedin 2007); more rapid transformation of organic nitrogen to mobile DIN (Ågren and Andersson 2012; Castellano and others 2012); enhanced chemical weathering rates (Drever 1982); and deeper flowpaths, through mineral soil horizons and fractured bedrock (Anderson and Dietrich 2001; Emili and Price 2013; Riebe and others 2016). How-

ever, the rainshadow watersheds also had higher proportions of early- and mid-seral forest cover (Figure S4) indicating potential for confounding forestry effects (Shah and others 2022; Pike and others 2010) and Alder cover with climatic effects. For example, greater relative cover of younger seral stages in previously logged watersheds of Oregon has been associated with higher stream nitrate concentrations and a lower DON % of TDN, potentially due to Alder (Cairns and Lajtha 2005).

In addition to climate and topography, and some associated watershed characteristics, a number of other factors could contribute to the spatial pattern of riverine water quality here and in other rainforest fjordlands. These include watershed size (for example, Laudon and Sponseller 2018), precipitation inputs of marine salts (Aherne and others 2010; Drever, 1982), and watershed geology (Jansen and others 2010; Li and others 2021). For example, carbonate rocks are highly soluble and contribute to elevated dissolved solutes in rivers (Milliman and Farnsworth 2011; Tank and others 2012a), probably including our Glacierized watershed type which had the most mixed-sedimentary bedrock (Table S1). Weathering of nitrogen-bearing rock is an historically underappreciated source of nitrogen to streams, particularly from rocks of sedimentary origin (Holloway and Dahlgren 2002) and mountainous areas (Houlton and others 2018). The age and composition of plutonic rock also varies geographically across our study area, becoming more felsic to the east (for example, Cecil and others 2018). Anadromous salmon are a potential source of marine derived nitrogen to streams (Hood and Berner 2009; Moore and others 2007; Sugai and Burrell 1984).

Several aspects of forestry can impact water quality, such as increased nitrate concentrations after harvesting or fertilizer applications (Shah and others 2022; Pike and others 2010). New research is needed to isolate the potential effects of commercial logging from climatic factors in this study area. More broadly, we have limited understanding of forestry effects across the diverse watersheds, logging histories, natural disturbance regimes, silvicultural practices, and evolving management paradigms of this area. Our study underscores the importance of controlling for meso-scale topo-climatic gradients when evaluating forestry effects on water quality.

Consequences of Spatial Heterogeneity in Water Quality

The large spatial heterogeneity of riverine water quality reported in this study likely has diverse local scale consequences for freshwater ecosystems and the land–ocean aquatic continuum (Xenopoulos and others 2017). Our findings suggest watershed classification can be used as a tool to conceptualize this heterogeneity in the form of a spatial mosaic of watershed ecosystems, as we have demonstrated for rainforest fjordlands in the NPCTR region (Figure 8; Figure 1). From a landscape ecology perspective, the water quality regime of rain-fed watersheds is distributed across a large number of small spatial units within the mosaic (Table S3). At the other extreme, the water quality regime of glacierized watersheds is found in a small number of large spatial units. The distribution of snow-type watersheds is intermediate between these two extremes.

Within the fjordland mosaic, streams of the Northern Rain Hills and Rain Lowlands—and to a lesser degree the Central Rain Mountains—are quite acidic, poorly buffered, warm, high in terrestrial DOM-associated solutes, and low in inorganic nutrients. Such a distinct water quality regime should affect freshwater community structure (Milner and others 2017; Petrin and others 2007) and nearshore ecosystem processes. Concentrated DOM-associated solutes provide an energy source that can be used by heterotrophs (St. Pierre and others 2020) and organic nitrogen that can be remineralized and used by primary producers. As a result, we expect that river plumes emanating from these watersheds function as heterotrophic (*biogeochemical*) *hotspots* (McClain and others 2003)—particularly during periods of high runoff (Oliver and others 2017; St. Pierre and others 2020); that is, these are *activated ecosystem control points* (Berhhardt and others 2017). On the other hand, the runoff from these watershed types is known to dilute the concentrations of inorganic nutrients directly used by primary producers (St. Pierre and others 2021). Our meso-scale analysis suggests that Rain type watersheds were an important cumulative source of water (33% of discharge) and must represent a large cumulative flux of organic matter associated materials (DOC, DON, Fe, and Al^{3+}).

In contrast with the Rain type watersheds, the larger Glacierized Mountain watersheds had the coolest and most turbid waters in the summer meltwater season (Figure 8). These physical aspects of runoff from glacierized watersheds affect multiple trophic levels in freshwater and nearshore ecosystems (for example, Bellmore and others 2022; Bianchi and others 2020; Milner and others 2017; Slemmons and others 2013). High particle loads make glacierized fjords such as Bute Inlet (Hage and others 2022) global hotspots for carbon

burial in bottom sediments (Smith and others 2015). The GMM type had the most buffered carbonate system, but would still contribute to the freshwater reductions in marine buffering capacity (Hare and others 2020) and the ecological impact of ocean acidification (Evans and others 2014; Tank and others 2012b). Nutrients in the runoff from glacierized mountains also influence ecosystems across the land to ocean aquatic continuum, but the effect of nutrients on marine productivity is uncertain and spatially variable, potentially depending on river turbidity, flow, temperature, and water column stratification (Bianchi and others 2020; Cuevas and others 2019; Hopwood and others 2020; Vargas and others 2011). Despite low concentrations of DOC and DON, glacial runoff here (St. Pierre and others 2022) and elsewhere (Arimitsu and others 2018; Vargas and others 2011) is thought to subsidize marine foodwebs due to high volume influxes of dilute but labile organic matter (Hood and others 2009).

Glacierized Mountain type watersheds probably dominate the overall land–ocean signature in these fjords due to their large cumulative area (50% of total) and discharge (44% of total), yet their importance is expected to vary across the larger fjordland complexes (for example, Pickard 1961) and over time. With rapid climate change, rates of glacier mass loss in this area are increasing dramatically and expected to peak in the coming decades before falling below current levels before the end of this century (Rounce and others 2023; Menounos, pers. comm.). Glacial influences on rivers and fjords of the NPCTR could be predicted to follow a similar long term trend (see Hood and Berner 2009; Bidlack and others 2021; Pitman and others 2020). However, the trajectory of water quality change may be complicated by other factors including the persistent physiographic setting, changing precipitation regimes (Wang and others 2016), changes in species composition (for example, Milner and others 2007), very long geomorphic and ecological lags (Anderson 2007; Church and Slaymaker 1989), and infrequent extreme events such as glacial lake outburst floods (Geertsema and others 2022).

Meso-scale Functions of Watershed Diversity?

The presence of such diversity in watershed ecosystems along the coastal margin supports the use of landscape ecology theory to better understand how land–sea linkages are expressed in meso-scale spatial units (for example, a fjord, an archipelago, or a fjordland complex). Consistent with the meta-ecosystem concept (Loreau and others 2003; Gounand and others 2018), coastal watershed ecosystems and nearshore ecosystems are indeed connected by multiple types of spatial flows in both upstream and downstream directions (for example, Aufdenkampe and others 2011; Harding and Reynolds 2014; Harding and others 2015; Moore and others 2007; Xenopoulos and others 2017). The fjordland complex between Rivers Inlet and Calvert Island, specifically, has been described as an *integrated land–ocean meta-ecosystem* due to the contributions of watershed, nearshore-macrophyte, and marine phytoplankton sources to the pool of particulate organic carbon found in the ocean surface waters (St. Pierre and others 2022 p. 2).

New research is needed to determine how the mosaic of interconnected watershed ecosystems and nearshore ecosystems in a given area determines meso-scale ecosystem functions and how those functions can be modeled. For example, higher diversity of watershed types can confer meso-scale resilience (for example, to salmon populations) due to habitat diversity (Hilborn and others 2003) and environmental asynchrony (Moore and others 2015). Nearshore nutrient stoichiometry and turbidity must depend on the mixing of diverse watershed sources from surrounding areas. Ocean acidification and oxygen depletion exemplify processes that can depend on both coastal ocean conditions and the flow of freshwater, organic matter, and rock weathering products from watersheds (Aufdenkampe and others 2011; Jackson and others 2021; Waldsbusser and others 2014). *Watershed classification for hydro-biogeochemistry* (Giesbrecht and others 2022), if coupled with coastal ocean modeling, offers a conceptual framework and geospatial tool for future studies to evaluate hypotheses about integrated land–ocean meta-ecosystems.

CONCLUSION

We conclude that watershed characterization and classification are useful tools for understanding complex spatial gradients and interacting catchment controls on multiple aspects of water quality in rainforest fjordlands. This approach suggested that the physiographic complexity of fjordland regions generates strong spatial gradients in watershed climate, topography, hydrology, and ecosystems. Most fjord studies focus on the few comparatively large (often glacierized) watersheds that tend to dominate discharge. However, this study described very different watershed ecosystem

characteristics in the many smaller catchments found across the broader fjordland complex. Where physiographic controls prevail, we would also expect to find diverse mosaics of watershed ecosystems in the extensive fjordland–island complexes around the world (Bianchi and others 2020). Steep spatial gradients in riverine water quality have potential implications for biological diversity and ecosystem processes at multiple scales in both freshwater and coastal ocean settings. Future research might ask how the biogeochemical and ecological processes of contrasting fjords depend on the mosaic of contributing watershed types. Such land–sea linkages are also expected to be influenced by oceanographic processes (for example, currents and mixing) operating at multiple scales.

Small ($< 10{,}000$ km^2) coastal mountain watersheds have been recognized for their disproportionate contributions to land-to-sea fluxes at global (Milliman and Syvitski, 1992; Lyons and others 2002) and regional scales (Goñi and others 2013; McNicol and others 2023). This study showed that small coastal watersheds can be highly diverse in terms of watershed characteristics and riverine water quality, even at meso-scales within the same climatic, physiographic, and geological region (that is, the Northeast Pacific Coastal Temperate Rainforest and the Coast Plutonic Complex). More work is needed at regional and global scales to understand the effects of many diverse small watersheds on the coastal ocean in comparison to the effects of few large watersheds (for example, the Fraser River in this region). Extending the small coastal watersheds concept to better account for spatial heterogeneity may lead to improved predictive and conceptual models of coastal margin function.

DATA AVAILABILITY

The datasets for this study can be found at: https://doi.org/10.5061/dryad.qv9s4mwp6.

OPEN ACCESS

REFERENCES

AdaptWest Project. 2020. Gridded current and projected climate data for North America at 1km resolution, generated using the ClimateNA v6.22 software (T. Wang and other 2020). Available at https://adaptwest.databasin.org/

Ågren GI, Andersson FO. 2012. Terrestrial ecosystem ecology: principles and applications. Cambridge: Cambridge University Press.

Aherne J, Mongeon A, Watmough SA. 2010. Temporal and spatial trends in precipitation chemistry in the Georgia Basin, British Columbia. J Limnol 69(1):4–10. https://doi.org/10.3274/JL10-69-S1-02.

Aitkenhead-Peterson JA, Alexander JE, Clair TA. 2005. Dissolved organic carbon and dissolved organic nitrogen export from forested watersheds in Nova Scotia: identifying controlling factors. Global Biogeochem Cycles 19(4):1–8. https://doi.org/10.1029/2004GB002438.

Alaback PB. 1996. Biodiversity patterns in relation to climate: The coastal temperate rainforests of North America. In: Lawford RG, Fuentes E, Alaback B, Eds. High-latitude rainforests and associated ecosystems of the west coast of the Americas: climate, hydrology, ecology, and conservation. New York: Springer.

Albers S. 2017. tidyhydat: extract and tidy Canadian hydrometric data. J Open Sour Softw 2(20):511. https://doi.org/10.21105/joss.00511.

Anderson SP. 2007. Biogeochemistry of glacial landscape systems. Ann Rev Earth Planet Sci 35:375–399. https://doi.org/10.1146/annurev.earth.35.031306.140033.

Anderson SP, Dietrich WE. 2001. Chemical weathering and runoff chemistry in a steep headwater catchment. Hydrol Process 15(10):1791–1815. https://doi.org/10.1002/hyp.240.

Anderson SP, Blanckenburg F. Von, White AF. 2007. Physical and chemical controls on the critical zone. Elements 3:315–319.

Arimitsu ML, Hobson KA, Webber DN, Piatt JF, Hood EW, Fellman JB. 2018. Tracing biogeochemical subsidies from glacier runoff into Alaska's coastal marine food webs. Global Change Biol 24(1):387–398. https://doi.org/10.1111/gcb.13875.

Aufdenkampe AK, Mayorga E, Raymond PA, Melack JM, Doney SC, Alin SR, Yoo K. 2011. Riverine coupling of biogeochemical cycles between land, oceans, and atmosphere. Front Ecol Environ 9(1):53–60. https://doi.org/10.1890/100014.

Banner A, LePage P, Moran J, de Groot A. 2005. The HyP3 project: pattern, process, and productivity in hypermaritime forests of Coastal British Columbia: a synthesis of 7-year results. Retrieved from http://www.for.gov.bc.ca/hfd/pubs/docs/srs/Srs10.pdf

Bellmore JR, Fellman JB, Hood E, Dunkle MR, Edwards RT. 2022. A melting cryosphere constrains fish growth by synchronizing the seasonal phenology of river food webs. Global Change Biol. https://doi.org/10.1111/gcb.16273.

Benner J, Lertzman K. 2022. Policy interventions and competing management paradigms shape the long-term distribution of forest harvesting across the landscape. Proc Nat Acad Sci 119(41):e2208360119. https://doi.org/10.1073/pnas.2208360119.

Bianchi TS, Arndt S, Austin WEN, Benn DI, Bertrand S, Cui X, Syvitski J. 2020. Fjords as aquatic critical zones (ACZs). Earth-Sci Rev 203(103145):1–25. https://doi.org/10.1016/j.earscirev.2020.103145.

Bidlack AL, Bisbing SM, Buma BJ, Diefenderfer HL, Fellman JB, Floyd WC, Ken P. 2021. Climate-mediated changes to linked terrestrial and marine ecosystems across the Northeast Pacific coastal temperate rainforest margin. BioScience 71(6):581–595. https://doi.org/10.1093/biosci/biaa171.

Bormann FH, Likens GE. 1967. Nutrient cycling. Science 155(4027):424–429. https://doi.org/10.1126/science.155.3761.424.

Brahney J, Bothwell ML, Capito L, Gray CA, Null SE, Menounos B, Curtis PJ. 2021. Glacier recession alters stream water quality characteristics facilitating bloom formation in the benthic diatom *Didymosphenia geminata*. Sci Total Environ 764:142856. https://doi.org/10.1016/j.scitotenv.2020.142856.

Breiman L. 2001. Random forests. Mach Learn 45:5–32. https://doi.org/10.1023/A:1010933404324.

Cairns MA, Lajtha K. 2005. Effects of succession on nitrogen export in the west-central cascades, oregon. Ecosystems 8(5):583–601. https://doi.org/10.1007/s10021-003-0165-5.

Castellano MJ, Lewis DB, Andrews DM, McDaniel MD. 2012. Coupling biogeochemistry and hydropedology to advance carbon and nitrogen cycling science. In: Lin H, Ed. Hydropedology: Synergistic integration of soil science and hydrology, . Amsterdam: Elsevier.

Cecil MR, Rusmore ME, Gehrels GE, Woodsworth GJ, Stowell HH, Yokelson IN, Homan E. 2018. Along-strike variation in the magmatic tempo of the Coast Mountains Batholith, British Columbia, and implications for processes controlling episodicity in arcs. Geochem, Geophys, Geosys 19(11):4274–4289. https://doi.org/10.1029/2018GC007874.

Chorover J, Derry LA, McDowell WH. 2017. Concentration-discharge relations in the critical zone: Implications for resolving critical zone structure, function, and evolution. Water Resour Res 53(11):8654–8659. https://doi.org/10.1002/2017WR021111.

Church M, Slaymaker O. 1989. Disequilibrium of Holocene sediment yield in glaciated British Columbia. Nature 337(6206):452–454. https://doi.org/10.1038/337452a0.

Colombo N, Bocchiola D, Martin M, Confortola G, Salerno F, Godone D, Freppaz M. 2019. High export of nitrogen and dissolved organic carbon from an Alpine glacier (Indren Glacier, NW Italian Alps). Aquat Sci 81(4):1–13. https://doi.org/10.1007/s00027-019-0670-z.

Compton JE, Church MR, Larned ST, Hogsett WE. 2003. Nitrogen export from forested watersheds in the Oregon Coast Range: The role of N2-fixing red alder. Ecosystems 6(8):773–785. https://doi.org/10.1007/s10021-002-0207-4.

Covino TP, McGlynn BL. 2007. Stream gains and losses across a mountain-to-valley transition: Impacts on watershed hydrology and stream water chemistry. Water Resour Res 43(10):1–14. https://doi.org/10.1029/2006WR005544.

Cuevas LA, Tapia FJ, Iriarte JL, González HE, Silva N, Vargas CA. 2019. Interplay between freshwater discharge and oceanic waters modulates phytoplankton size-structure in fjords and channel systems of the Chilean Patagonia. Prog Oceanogr 173:103–113. https://doi.org/10.1016/j.pocean.2019.02.012.

Cui Y, Miller D, Schiarizza P, Diakow LJ. 2017. *British Columbia digital geology*. British Columbia Ministry of Energy, Mines and Petroleum Resources, British Columbia Geological Survey Open File 20178, 9p. Data version 2018–04–05. Retrieved from: https://www2.gov.bc.ca/gov/content/industry/mineral-exploration-mining/british-columbia-geological-survey/geology/bcdigitalgeology

Curran JH, Biles FE. 2021. Identification of seasonal streamflow regimes and streamflow drivers for daily and peak flows in Alaska. Water Resourc Res. https://doi.org/10.1029/2020wr028425.

D'Amore DV, Edwards RT, Herendeen PA, Hood E, Fellman JB. 2015. Dissolved organic carbon fluxes from hydropedologic

units in Alaskan coastal temperate rainforest watersheds. Soil Sci Soc Am J 79:378–388. https://doi.org/10.2136/sssaj2014.09.0380.

Demarchi, D. A. 2011. *An introduction to the Ecoregions of British Columbia*. Ministry of Environment. Retrieved from http://www.env.gov.bc.ca/wld/documents/techpub/rn324.pdf

Dick A (Kwaxsistalla Wathl'thla), Sewid-Smith D (Mayanilth), Recalma-Clutesi K (Oqwilowgwa), Deur D (Moxmowisa), Turner NJ (Galitsimġa). 2022. ''From the beginning of time'': The colonial reconfiguration of native habitats and Indigenous resource practices on the British Columbia Coast. FACETS 7:543–570. https://doi.org/10.1139/facets-2021-0092

Drever JI. 1982. The geochemistry of natural waters: Surface and groundwater environments (Third). New Jersey: Prentice-Hall.

Edwards RT, D'Amore DV, Biles FE, Fellman JB, Hood EW, Trubilowicz JW, Floyd WC. 2021. Riverine dissolved organic carbon and freshwater export in the Eastern Gulf of Alaska. J Geophys Res: Biogeosci 126(1):1–16. https://doi.org/10.1029/2020jg005725.

Emili LA, Price JS. 2013. Biogeochemical processes in the soil-groundwater system of a forest-peatland complex, North Coast British Columbia Canada. Northwest Sci 87(4):326–348. https://doi.org/10.3955/046.087.0406.

EPA. 2000. Guidance for data quality assessment (No. EPA QA/G-9 QA00 Version). Environmental Protection Agency.

Esri. 2020. ArcGIS Desktop. Redlands, CA. https://esri.com

Evans W, Mathis JT, Cross JN. 2014. Calcium carbonate corrosivity in an Alaskan inland sea. Biogeosciences 11(2):365–379. https://doi.org/10.5194/bg-11-365-2014.

Fellman JB, Hood E, Edwards RT, D'Amore DV. 2009. Changes in the concentration, biodegradability, and fluorescent properties of dissolved organic matter during stormflows in coastal temperate watersheds. J Geophys Res: Biogeosci 114(1):1–14. https://doi.org/10.1029/2008JG000790.

Fellman JB, Hood E, Spencer RGM, Stubbins A, Raymond PA. 2014a. Watershed glacier coverage influences dissolved organic matter biogeochemistry in coastal watersheds of Southeast Alaska. Ecosystems 17:1014–1025. https://doi.org/10.1007/s10021-014-9777-1.

Fellman JB, Nagorski S, Pyare S, Vermilyea A, Scott D, Hood E. 2014b. Stream temperature response to variable glacier coverage in coastal watersheds of Southeast Alaska. Hydrol Process 28:2062–2073.

Fellman JB, Hood E, D'Amore DV, Edwards RT. 2021. Streamflow variability controls N and P export and speciation from Alaskan coastal temperate rainforest watersheds. Biogeochemistry. https://doi.org/10.1007/s10533-020-00752-w.

Fitzgerald DF, Price JS, Gibson JJ. 2003. Hillslope-swamp interactions and flow pathways in a hypermaritime rainforest British Columbia. Hydrol Process 17(15):3005–3022. https://doi.org/10.1002/hyp.1279.

Gaillardet J, Dupre B, Louvat P, Allegre CJ. 1999. Global silicate weathering and CO2 consumption rates deduced from the chemistry of large rivers. Chem Geol 159(8):3–30. https://doi.org/10.1016/S0009-2541(99)00031-5.

Garrity CP, Soller DR (2009) Database of the Geologic Map of North America; adapted from the map by J.C. Reed, Jr. and others. U.S. Geological Survey Data Series 424. Retrieved from: http://pubs.usgs.gov/ds/424/

Geertsema M, Menounos B, Bullard G, Carrivick JL, Clague JJ, Dai C, Donati D, Ekstrom G, Jackson JM, Lynett P, Pichierri M, Pon A, Shugar DH, Stead D, Del Bel Belluz J, Friele P, Giesbrecht I, Heathfield D, Millard T, Nasonova S, Schaeffer AJ, Ward BC, Blaney D, Blaney E, Brillon C, Bunn C, Floyd W, Higman B, Hughes KE, McInnes W, Mukherjee K, Sharp MA. 2022. The 28 November 2020 landslide, tsunami, and outburst flood—A hazard cascade associated with rapid deglaciation at Elliot Creek, British Columbia, Canada. Geophys Res Lett. https://doi.org/10.1029/2021GL096716.

GeoBC (2008) Freshwater atlas lakes. Retrieved from: https://catalogue.data.gov.bc.ca/dataset/freshwater-atlas-lakes

GeoBC (2009) Freshwater atlas assessment watersheds. Retrieved from: https://catalogue.data.gov.bc.ca/dataset/97d8ef37-b8d2-4c3b-b772-6b25c1db13d0

GeoBC (2014) Digital elevation model for British Columbia – CDED – 1:250,000. Retrieved from: https://catalogue.data.gov.bc.ca/dataset/7b4fef7e-7cae-4379-97b8-62b03e9ac83d

Gibbs RJ. 1970. Mechanisms controlling world water chemistry. Science 170(3962):1088–1090.

Gibson JJ, Price JS, Aravena R, Fitzgerald DF, Maloney D. 2000. Runoff generation in a hypermaritime bog–forest upland. Hydrol Process 14(15):2711–2730.

Giesbrecht IJW, Tank SE, Frazer GW, Hood E, Gonzalez Arriola SG, Butman DE, Lertzman KP. 2022. Watershed classification predicts streamflow regime and organic carbon dynamics in the Northeast Pacific Coastal Temperate Rainforest. Global Biogeochem Cycles 36(2):1–27. https://doi.org/10.1029/2021gb007047.

Goñi MA, Hatten JA, Wheatcroft RA, Borgeld JC. 2013. Particulate organic matter export by two contrasting small mountainous rivers from the Pacific Northwest, U.S.A. J Geophys Res: Biogeosci 118:112–134. https://doi.org/10.1002/jgrg.20024.

Gounand I, Harvey E, Little CJ, Altermatt F. 2018. Meta-ecosystems 20: rooting the theory into the field. Trends Ecol Evolut 33(1):36–46. https://doi.org/10.1016/j.tree.2017.10.006.

Hage S, Galy VV, Cartigny MJB, Heerema C, Heijnen MS, Acikalin S, … Talling PJ. 2022. Turbidity currents can dictate organic carbon fluxes across river–fed fjords: An example from Bute Inlet (BC, Canada). J Geophys Res: Biogeosci 1–16. https://doi.org/10.1029/2022jg006824.

Harding JMS, Segal MR, Reynolds JD. 2015. Location is everything: Evaluating the effects of terrestrial and marine resource subsidies on an estuarine bivalve. PLoS ONE 10(5):1–25. https://doi.org/10.1371/journal.pone.0125167.

Harding JMS, Reynolds JD. 2014. From earth and ocean: investigating the importance of cross-ecosystem resource linkages to a mobile estuarine consumer. Ecosphere 5(5):1–23. https://doi.org/10.1890/ES14-00029.1.

Hare A, Evans W, Pocock K, Weekes C, Gimenez I. 2020. Contrasting marine carbonate systems in two fjords in British Columbia, Canada: seawater buffering capacity and the response to anthropogenic CO2 invasion. PloS One 15(9):e0238432. https://doi.org/10.1371/journal.pone.0238432.

Hartmann J, Moosdorf N. 2012. The new global lithological map database GLiM: a representation of rock properties at the Earth surface. Geochem, Geophys, Geosyst 13(12):1–37. https://doi.org/10.1029/2012GC004370.

Hartmann J, Moosdorf N, Lauerwald R, Hinderer M, West AJ. 2014. Global chemical weathering and associated P-release - the role of lithology, temperature and soil properties. Chem

Geol 363:145–163. https://doi.org/10.1016/j.chemgeo.2013.10.025.

Hember RA. 2018. Spatially and temporally continuous estimates of annual total nitrogen deposition over North America, 1860–2013. Data in Brief 17:134–140. https://doi.org/10.1016/j.dib.2017.12.052.

Hilborn R, Quinn TP, Schindler DE, Rogers DE. 2003. Biocomplexity and fisheries sustainability. Proc Nat Acad Sci United States Am 100(11):6564–6568. https://doi.org/10.1073/pnas.1037274100.

Hodgkins R, Tranter M, Dowdeswell JA. 1997. Solute provenance, transport and denudation in a High Arctic glacierized catchment. Hydrol Process 11(14):1813–1832. https://doi.org/10.1002/(sici)1099-1085(199711)11:14%3c1813::aid-hyp498%3e3.0.co;2-c.

Hodson, A., Anesio, A. M., Tranter, M., Fountain, A., Osborn, M., Priscu, J., … Sattler, B. (2008). Glacial ecosystems. Ecological Monographs. https://doi.org/10.1890/07-0187.1

Hoffman KM, Lertzman KP, Starzomski BM. 2017. Ecological legacies of anthropogenic burning in a British Columbia coastal temperate rain forest. J Biogeogr 44(12):2903–2915. https://doi.org/10.1111/jbi.13096.

Holloway JAM, Dahlgren RA. 2002. Nitrogen in rock: occurrences and biogeochemical implications. Global Biogeochem Cycles. https://doi.org/10.1029/2002GB001862.

Hood E, Berner L. 2009. Effects of changing glacial coverage on the physical and biogeochemical properties of coastal streams in southeastern Alaska. J Geophys Res 114:1–10. https://doi.org/10.1029/2009JG000971.

Hood E, Fellman J, Spencer RGM, Hernes PJ, Edwards R, Damore D, Scott D. 2009. Glaciers as a source of ancient and labile organic matter to the marine environment. Nature 462(7276):1044–1047. https://doi.org/10.1038/nature08580.

Hopwood MJ, Carroll D, Dunse T, Hodson A, Holding JM, Iriarte JL, Meire L. 2020. Review article: How does glacier discharge affect marine biogeochemistry and primary production in the Arctic? Cryosphere 14(4):1347–1383.

Houlton BZ, Morford SL, Dahlgren RA. 2018. Convergent evidence for widespread rock nitrogen sources in Earth's surface environment. Science 360:58–62. https://doi.org/10.1126/science.aan4399.

Jackley J, Gardner L, Djunaedi AF, Salomon AK. 2016. Ancient clam gardens, traditional management portfolios, and the resilience of coupled human-ocean systems. Ecol Soc. https://doi.org/10.5751/ES-08747-210420.

Jackson JM, Johannessen S, Del Bel Belluz J, Hunt BPV, Hannah CG. 2021. Identification of a seasonal subsurface oxygen minimum in Rivers Inlet, British Columbia. Estuaries and Coasts. https://doi.org/10.1007/s12237-021-00999-y.

Jansen N, Hartmann J, Lauerwald R, Dürr HH, Kempe S, Loos S, Middelkoop H. 2010. Dissolved silica mobilization in the conterminous USA. Chem Geol 270(1–4):90–109. https://doi.org/10.1016/j.chemgeo.2009.11.008.

Korver MC, Haughton E, Floyd WC, Giesbrecht IJW. 2022. High-resolution streamflow and weather data (2013–2019) for seven small coastal watersheds in the northeast Pacific coastal temperate rainforest, Canada. Earth Syst Sci Data 14:4231–4250. https://doi.org/10.5194/essd-14-4231-2022.

Laudon H, Sponseller RA. 2018. How landscape organization and scale shape catchment hydrology and biogeochemistry: insights from a long-term catchment study. Wires Water. https://doi.org/10.1002/wat2.1265.

Levin SA. 1992. The problem of pattern and scale in ecology. Ecology 73(6):1943–1967. https://doi.org/10.2307/1941447.

Li L, Sullivan PL, Benettin P, Cirpka OA, Bishop K, Brantley SL, Kirchner JW. 2021. Toward catchment hydro-biogeochemical theories. Wiley Interdiscip Rev: Water 8(1):1–31. https://doi.org/10.1002/wat2.1495.

Liaw A, Wiener M. 2002. Classification and regression by random forest. R News 2(3):18–22.

Likens GE. 2001. Biogeochemistry, the watershed approach: some uses and limitations. Mar Freshw Res 52(1):5–12. https://doi.org/10.1071/MF99188.

Lintern A, Webb JA, Ryu D, Liu S, Waters D, Leahy P, Western AW. 2018. What are the key catchment characteristics affecting spatial differences in riverine water quality? Water Resour Res 54(10):7252–7272.

Loreau M, Mouquet N, Holt RD. 2003. Meta-ecosystems: A theoretical framework for a spatial ecosystem ecology. Ecol Lett 6(8):673–679. https://doi.org/10.1046/j.1461-0248.2003.00483.x.

Lyons WB, Nezat CA, Carey AE, Hicks DM. 2002. Organic carbon fluxes to the ocean from high-standing islands. Geology 30(5):443–446. https://doi.org/10.1130/0091-7613(2002)030%3c0443:OCFTTO%3e2.0.CO;2.

McClain ME, Boyer EW, Dent CL, Gergel SE, Grimm NB, Groffman PM, Pinay G. 2003. Biogeochemical hot spots and hot moments at the interface of terrestrial and aquatic ecosystems. Ecosystems 6(4):301–312. https://doi.org/10.1007/s10021-003-0161-9.

McDowell WH, Wood T. 1984. Podzolization: soil processes control dissolved organic carbon concentrations in stream water. Soil Sci 137(1):23–32.

McLaren D, Fedje D, Dyck A, Mackie Q, Gauvreau A, Cohen J. 2018. Terminal pleistocene epoch human footprints from the Pacific coast of Canada. PLoS ONE 13(3):12–15. https://doi.org/10.1371/journal.pone.0193522.

McNicol G, Bulmer C, D'Amore D, Sanborn P, Saunders S, Giesbrecht I, Arriola SG, Bidlack A, Butman D, Buma B. 2019. Large, climate-sensitive soil carbon stocks mapped with pedology-informed machine learning in the North Pacific coastal temperate rainforest. Environ Res Lett 14(1):014004. https://doi.org/10.1088/1748-9326/aaed52.

McNicol G, Hood E, Butman DE, Tank SE, Giesbrecht IJW, Floyd W, D'Amore D, Fellman JB, Cebulski A, Lally A, McSorley H, Gonzalez Arriola SG. 2023. Small, coastal temperate rainforest watersheds dominate dissolved organic carbon transport to the Northeast Pacific Ocean. Geophys Res Lett. https://doi.org/10.1029/2023GL103024.

Meidinger D, Pojar J. 1991. Ecosystems of British Columbia. (D. Meidinger & J. Pojar, Eds.), Special Report Series 6. Victoria, BC: Research Branch BC Ministry of forests. Retrieved from https://www.for.gov.bc.ca/hfd/pubs/docs/srs/srs06.htm

Mendoza-Lera C, Catalán N, Lupon A. 2021. Editorial: Watershed and stream: the inseparable functional/biogeochemical unit. Front Water 3:1–2. https://doi.org/10.3389/frwa.2021.801389.

Meybeck M. 1982. Carbon, nitrogen, and phosphorous transport by world rivers. Am J Sci 282:401–450.

Milliman JD, Farnsworth KL. 2011. River discharge to the coastal ocean: a global synthesis. Cambridge: Cambridge University Press. https://doi.org/10.1017/CBO9780511781247.

Milliman JD, Syvitski JPM. 1992. Geomorphic / tectonic control of sediment discharge to the ocean: the importance of small mountainous rivers. J Geol 100(5):525–544. https://doi.org/10.1086/629606.

Milner AM, Fastie CL, Chapin FS, Engstrom DR, Sharman LC. 2007. Interactions and linkages among ecosystems during landscape evolution. BioScience 57(3):237–247. https://doi.org/10.1641/b570307.

Milner AM, Khamis K, Battin TJ, Brittain JE, Barrand NE, Füreder L, Brown LE. 2017. Glacier shrinkage driving global changes in downstream systems. Proc Nat Acad Sci United States Am 114(37):9770–9778. https://doi.org/10.1073/pnas.1619807114.

Moore JW, Schindler DE, Carter JL, Fox J, Griffiths J, Holtgrieve GW. 2007. Biotic control of stream fluxes: Spawning salmon drive nutrient and matter export. Ecology 88(5):1278–1291. https://doi.org/10.1890/06-0782.

Moore RD, Fleming SW, Menounos B, Wheate R, Fountain A, Stahl K, Jakob M. 2009. Glacier change in Western North America: influences on hydrology, geomorphic hazards and water quality. Hydrol Process 23:42–61. https://doi.org/10.1002/hyp.7162.

Moore JW, Beakes MP, Nesbitt HK, Yeakel JD, Patterson DA, Thompson LA, Atlas WI. 2015. Emergent stability in a large, free-flowing watershed. Ecology 96(2):340–347. https://doi.org/10.1890/14-0326.1.

Moosdorf N, Hartmann J (2015) Global Lithological Map (GLiM) database v1.1. Retrieved on March 12, 2018, from: https://ccgm.org/en/home/168-lithological-map-of-the-world-9782917310250.html

Mulholland PJ. 2003. Large-scale patterns in dissolved organic carbon concentration, flux, and sources. In: Findlay SEG, Sinsabaugh RL, Eds. Aquatic ecosystems: Interactivity of dissolved organic matter. Academic Press.

O'Neel S, Hood E, Bidlack AL, Fleming SW, Arimitsu ML, Arendt A, Pyare S. 2015. Icefield-to-ocean linkages across the northern pacific coastal temperate rainforest ecosystem. BioScience 65(5):499–512. https://doi.org/10.1093/biosci/biv027.

Old Growth Technical Advisory Panel Daust D, Price K, Holt R, Matthaus L, Merkel G 2021b Forest seral stage. GIS shapefile retrieved on January 26, 2022, from: https://catalogue.data.gov.bc.ca/dataset/old-growth-technical-advisory-panel-tap-forest-seral-stage

Old Growth Technical Advisory Panel (Daust D, Price K, Holt R, Matthaus L, Merkel G (2021a) Priority deferrals: an ecological approach. Retrieved from: https://www2.gov.bc.ca/assets/gov/farming-natural-resources-and-industry/forestry/stewardship/old-growth-forests/summary_for_g2g_package.pdf

Oliver AA, Tank SE, Giesbrecht I, Korver MC, Floyd WC, Sanborn P, Lertzman KP. 2017. A global hotspot for dissolved organic carbon in hypermaritime watersheds of coastal British Columbia. Biogeosciences 14:3743–3762. https://doi.org/10.5194/bg-14-3743-2017.

Ouellet Dallaire C, Lehner B, Sayre R, Thieme M. 2019. A multidisciplinary framework to derive global river reach classifications at high spatial resolution. Environ Res Lett. https://doi.org/10.1088/1748-9326/aad8e9.

Pearson AF. 2010. Natural and logging disturbances in the temperate rain forests of the Central Coast, British Columbia. Can J for Res 40(10):1970–1984. https://doi.org/10.1139/X10-137.

Perakis SS, Hedin LO. 2007. State factor relationships of dissolved organic carbon and nitrogen losses from unpolluted temperate forest watersheds. J Geophys Res: Biogeosci. https://doi.org/10.1029/2006JG000276.

Perakis SS, Hedin LO. 2002. Nitrogen loss from unpolluted South American forests mainly via dissolved organic compounds. Nature 415(6870):416–419. https://doi.org/10.1038/415416a.

Petrin Z, McKie B, Buffam I, Laudon H, Malmqvist B. 2007. Landscape-controlled chemistry variation affects communities and ecosystem function in headwater streams. Can J Fisher Aquat Sci 64(11):1563–1572. https://doi.org/10.1139/F07-118.

Pickard GL. 1961. Oceanographic features of inlets in the British Columbia Mainland Coast. J Fish Res Board Can 18(6):907–999.

Pickett STA, Cadenasso ML. 1995. Landscape ecology: spatial heterogeneity in ecological systems. Science 269(5222):331–334.

Pike RG, Feller MC, Stednick JD, Rieberger KJ, Carver M (2010) Water quality and forest management. Land Management Handbook 66, 401–440. BC Min. For. Range, Victoria, B.C. www.for.gov.bc.ca/hfd/pubs/Docs/Lmh/Lmh66.htm

Pitman KJ, Moore JW, Sloat MR, Beaudreau AH, Bidlack AL, Brenner RE, Whited DC. 2020. Glacier retreat and Pacific salmon. BioScience 70(3):220–236. https://doi.org/10.1093/biosci/biaa015.

Pojar J, Klinka K, Demarchi DA. 1991. Coastal Western Hemlock Zone. In: Meidinger D, Pojar J, Eds. Ecosystems of British Columbia. BC: Victoria. pp 95–111.

R Core Team (2020). R: A language and environment for statistical computing. R Foundation for Statistical Computing, Vienna, Austria. URL https://www.R-project.org/

Raymond PA, Saiers JE, Sobczak WV. 2016. Hydrological and biogeochemical controls on watershed dissolved organic matter transport: pulse-shunt concept. Ecology 97(1):5–16. https://doi.org/10.1890/14-1684.1.

Reid M, Collins ML, Hall SRJ, Mason E, McGee G, Frid A. 2022. Protecting our coast for everyone's future: Indigenous and scientific knowledge support marine spatial protections proposed by Central Coast First Nations in Pacific Canada. People Nat. https://doi.org/10.1002/pan3.10380.

Ren Z, Martyniuk N, Oleksy IA, Swain A, Hotaling S. 2019. Ecological stoichiometry of the mountain cryosphere. Front Ecol Evolut 7:1–16. https://doi.org/10.3389/fevo.2019.00360.

RGI Consortium (2017). Randolph Glacier Inventory – A Dataset of global glacier outlines: Version 6.0: Technical Report, Global Land Ice Measurements from Space, Colorado, USA. Digital Media. https://doi.org/10.7265/N5-RGI-60

Richter D, deB, & Billings, S. A. 2015. 'One physical system': Tansley's ecosystem as Earth's critical zone. New Phytol 206:900–912. https://doi.org/10.1111/nph.13338.

Riebe CS, Hahm WJ, Brantley SL. 2016. Controls on deep critical zone architecture: a historical review and four testable hypotheses. Earth Surf Process Landf. https://doi.org/10.1002/esp.4052.

Rounce DR, Hock R, Maussion F, Hugonnet R, Kochtitzky W, Huss M, McNabb RW. 2023. Global glacier change in the 21st century: Every increase in temperature matters. Science 379:78–83.

Rusmore ME, Woodsworth GJ. 1991. Coast plutonic complex: a mid-cretaceous contractional orogen. Geology 19(9):941–944.

Sanborn P, Lamontagne L, Hendershot W. 2011. Podzolic soils of Canada: genesis, distribution, and classification. Can J Soil Sci 91(5):843–880. https://doi.org/10.4141/cjss10024.

Schlesinger WH. 1997. Biogeochemistry: an analysis of global change, 2nd edn. San Diego: Academic Press.

Sergeant CJ, Sexton EK, Moore JW, Westwood AR, Nagorski SA, Ebersole JL,… Skuce N. 2022. Risks of mining to salmonid-bearing watersheds. Science Advances 8(26):eabn0929. Retrieved from https://doi.org/10.1126/sciadv.abn0929.

Shah NW, Baillie BR, Bishop K, Ferraz S, Högbom L, Nettles J. 2022. The effects of forest management on water quality. For Ecol Manag. https://doi.org/10.1016/j.foreco.2022.120397.

Simard M, Pinto N, Fisher JB, Baccini A. 2011. Mapping forest canopy height globally with spaceborne lidar. J Geophys Res 116(4):1–12. https://doi.org/10.1029/2011JG001708.

Slemmons KEH, Saros JE, Simon K. 2013. The influence of glacial meltwater on alpine aquatic ecosystems: a review. Environ Sci: Process Impacts 15(10):1794–1806. https://doi.org/10.1039/c3em00243h.

Slemmons KEH, Rodgers ML, Stone JR, Saros JE. 2017. Nitrogen subsidies in glacial meltwaters have altered planktonic diatom communities in lakes of the US Rocky Mountains for at least a century. Hydrobiologia 800(1):129–144. https://doi.org/10.1007/s10750-017-3187-2.

Smith RW, Bianchi TS, Allison M, Savage C, Galy V. 2015. High rates of organic carbon burial in fjord sediments globally. Nat Geosci 8(6):450–453. https://doi.org/10.1038/ngeo2421.

Snelder TH, Biggs BJF. 2002. Multiscale river environment classification for water resources management. J Am Water Resour Assoc 38(5):1225–1239. https://doi.org/10.1111/j.1752-1688.2002.tb04344.x.

Sobek S, Tranvik LJ, Prairie YT, Kortelainen P, Cole JJ. 2007. Patterns and regulation of dissolved organic carbon: an analysis of 7,500 widely distributed lakes. Limnol Oceanogr 52(3):1208–1219. https://doi.org/10.4319/lo.2007.52.3.1208.

St Pierre KA, Hunt BPV, Giesbrecht IJW, Tank SE, Lertzman KP, Del J, Froese T (2022) Seasonally and spatially variable organic matter contributions from watershed, marine macrophyte, and pelagic sources to the Northeast Pacific coastal ocean margin. Frontiers in Marine Science, 9(July), 1–17. https://doi.org/10.3389/fmars.2022.863209

St Pierre KA, Oliver AA, Tank SE, Hunt BPV, Giesbrecht I, Kellogg CTE, Korver MC. 2020. Terrestrial exports of dissolved and particulate organic carbon affect nearshore ecosystems of the Pacific coastal temperate rainforest. Limnol Oceanogr 65(11):2657–2675. https://doi.org/10.1002/lno.11538.

St Pierre K, Hunt B, Tank S, Giesbrecht I, Korver M, Floyd W, Lertzman K. 2021. Rain-fed streams dilute inorganic nutrients but subsidise organic-matter-associated nutrients in coastal waters of the northeast Pacific Ocean. Biogeosciences 18:3029–3052. https://doi.org/10.5194/bg-18-3029-2021.

Steinberg PD, Brett MT, Bechtold JS, Richey JE, Porensky LM, Smith SN. 2011. The influence of watershed characteristics on nitrogen export to and marine fate in Hood Canal, Washington, USA. Biogeochemistry 106(3):415–433. https://doi.org/10.1007/s10533-010-9521-7.

Stewart B, Shanley JB, Kirchner JW, Norris D, Adler T, Bristol C, Li L. 2021. Streams as mirrors: reading subsurface water chemistry from stream chemistry. Water Resour Res. https://doi.org/10.1029/2021wr029931.

Stowell HH. 2006. Geology of Southeast Alaska: Rock and ice in motion. Fairbanks: University of Alaska Press.

Sugai SF, Burrell DC. 1984. Transport of dissolved organic carbon, nutrients, and trace metals from the Wilson and Blossom rivers to Smeaton Bay, southeast Alaska. Can J Fish Aquat Sci 41(1):180–190. https://doi.org/10.1139/f84-019.

Tank SE, Frey KE, Striegl RG, Raymond PA, Holmes RM, McClelland JW, Peterson BJ. 2012a. Landscape-level controls on dissolved carbon flux from diverse catchments of the circumboreal. Global Biogeochem Cycles 26(3):1–15. https://doi.org/10.1029/2012GB004299.

Tank SE, Raymond PA, Striegl RG, McClelland JW, Holmes RM, Fiske GJ, Peterson BJ. 2012b. A land-to-ocean perspective on the magnitude, source and implication of DIC flux from major Arctic rivers to the Arctic Ocean. Global Biogeochem Cycles 26(4):1–15. https://doi.org/10.1029/2011GB004192.

Tank SE, Giesbrecht IJW, Oliver AO, St Pierre KA, Fedje B, Myers E, Quayle L, Desmarais I, McEwan S, Roberts N (2020) Biogeochemical sampling of streams in the Kwakshua Watersheds of Calvert and Hecate Islands, BC: 2013–2019. Version 1.0. Hakai Institute Data Package. https://doi.org/10.21966/7qnv-6y88

Thompson SD, Nelson TA, Giesbrecht I, Frazer G, Saunders SC. 2016. Data-driven regionalization of forested and non-forested ecosystems in coastal British Columbia with LiDAR and RapidEye imagery. Appl Geogr 69:35–50. https://doi.org/10.1016/j.apgeog.2016.02.002.

Tranter M, Wadham JL. 2014. Geochemical weathering in glacial and proglacial environments. Treatise on Geochemistry, . Elsevierpp 157–173. https://doi.org/10.1016/B978-0-08-095975-7.00505-2.

Turner MG. 1989. Landscape ecology: The effect of pattern on process. Ann Rev Ecol Syst 20(1):171–197. https://doi.org/10.1146/annurev.es.20.110189.001131.

Vargas CA, Martinez RA, San V, Aguayo M, Silva N, Torres R. 2011. Allochthonous subsidies of organic matter across a lake – river – fjord landscape in the Chilean Patagonia: implications for marine zooplankton in inner fjord areas. Cont Shelf Res 31(3–4):187–201. https://doi.org/10.1016/j.csr.2010.06.016.

Wang T, Hamann A, Spittlehouse D, Carroll C. 2016. Locally downscaled and spatially customizable climate data for historical and future periods for North America. PLoS ONE 11(6):1–17. https://doi.org/10.1371/journal.pone.0156720.

Warner KA, Saros JE, Simon KS. 2017. Nitrogen subsidies in glacial meltwater: implications for high elevation aquatic chains. Water Resour Res 53(11):9791–9806. https://doi.org/10.1002/2016WR020096.

White AF, Blum AE, Bullen TD, Vivit DV, Schulz M, Fitzpatrick J. 1999. The effect of temperature on experimental and natural chemical weathering rates of granitoid rocks. Geochimica et Cosmochimica Acta 63(19–20):3277–3291. https://doi.org/10.1016/S0016-7037(99)00250-1.

Wiens JA. 2002. Riverine landscapes: Taking landscape ecology into the water. Freshw Biol 47(4):501–515. https://doi.org/10.1046/j.1365-2427.2002.00887.x.

Williamson CE, Dodds W, Kratz TK, Palmer MA. 2008. Lakes and streams as sentinels of environmental change in terrestrial and atmospheric processes. Front Ecol Environ 6(5):247–254.

Wolf EC, Mitchell AP, Schoonmaker PK (1995) The rain forests of home: an atlas of people and place. Interrain, 31. Retrieved from http://www.ecotrust.org/publications/rain_forests_atlas.html

Wolock DM, Winter TC, McMahon G. 2004. Delineation and evaluation of hydrologic-landscape regions in the United States using geographic information system tools and multi-

variate statistical analyses. Environ Manag 34(1):71–88. https://doi.org/10.1007/s00267-003-5077-9.

Wood SN. 2011. Fast stable restricted maximum likelihood and marginal likelihood estimation of semiparametric generalized linear models. J R Stat Soc (b) 73(1):3–36.

Wood SN (2017) Generalized Additive Models: An Introduction with R (2nd edition). Chapman and Hall/CRC.

Xenopoulos MA, Downing JA, Kumar MD, Menden-Deuer S, Voss M. 2017. Headwaters to oceans: Ecological and biogeochemical contrasts across the aquatic continuum. Limno Oceanogr 62:S3–S14. https://doi.org/10.1002/lno.10721.